Supporting Information

Development of NIAD-4 Derivatives for Fluorescence-based Detection of Protein Aggregates

Tze Cin Owyong,[a] Laura E. Shippey,[a,b] Siyang Ding,[a] David S. Owen,[b] Shouxiang Zhang,[a] Jonathan M. White,[c] Wallace W.H. Wong,[c,d] David P. Smith[b] and Yuning Hong*[a]

a. Department of Biochemistry and Chemistry, La Trobe Institute for Molecular Science, La Trobe University, Melbourne, VIC 3086, Australia

b. Department of Biosciences and Chemistry, Sheffield Hallam University, Sheffield, United Kingdom

c. School of Chemistry, Bio21 Institute, The University of Melbourne, Parkville, VIC 3010, Australia

d. ARC Centre of Excellence in Exciton Science, The University of Melbourne, Parkville, VIC 3010 (Australia)

*Email: Y.Hong@latrobe.edu.au (Y.H.)

Contents

1. Synthesis Procedures and Characterisation

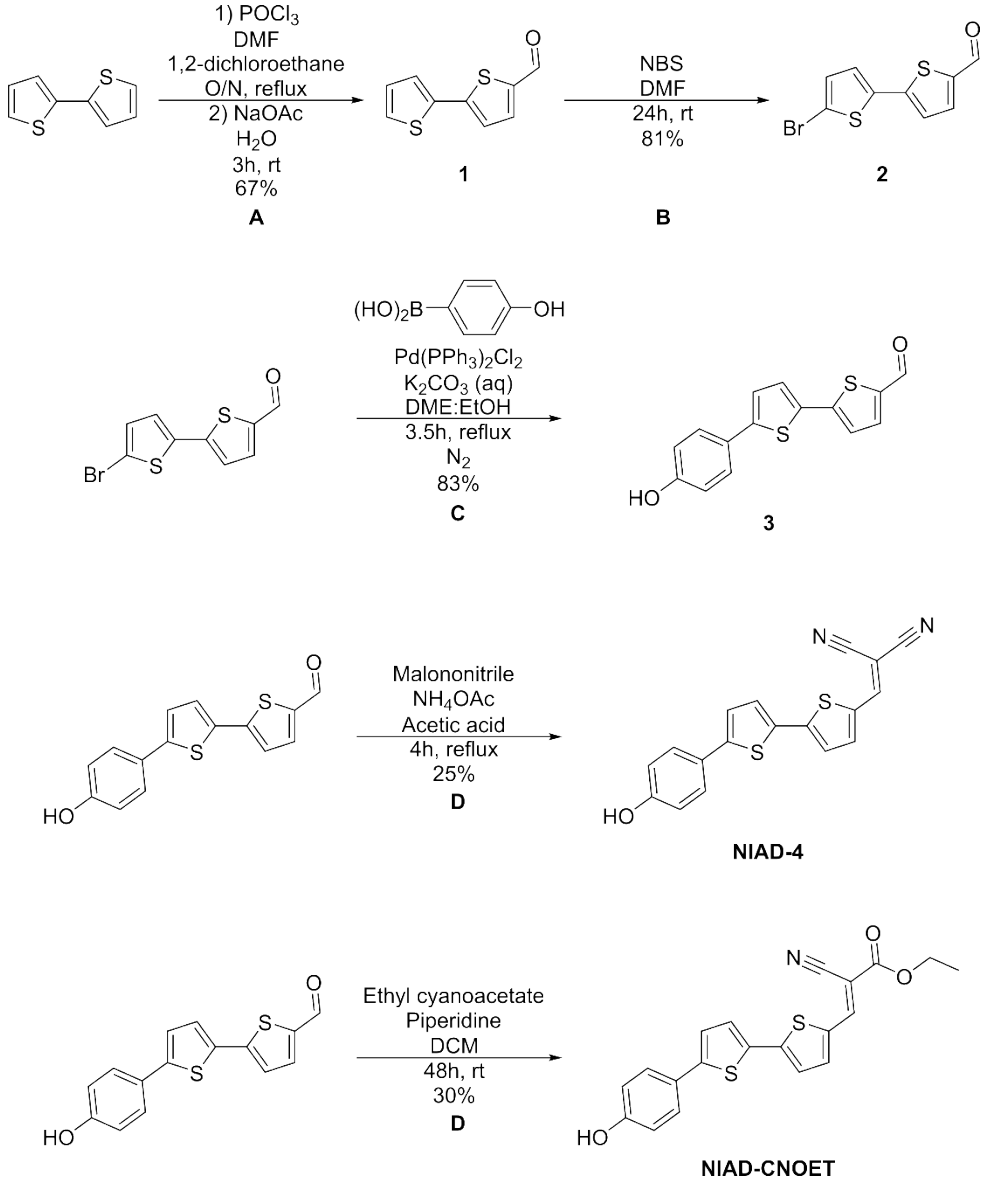

Scheme S1: Synthetic scheme for primary bithiophene **2**, **NIAD-4** and **NIAD-CNOET**. (A) Vilsmeier-Haack reaction. (B) Bromination with NBS. (C) Palladium catalysed Suzuki coupling. (D) Knoevenagel condensation.

2-Formyl-2,2'-bithiophene (1)

2,2'-Bithiophene (20.0 g, 120 mmol), DMF (8.80 g, 120 mmol) was added in 150 mL 1,2-dichloroethane stirred and cooled to 0 °C. $POCl_3$ (18.4 g, 120 mmol) was added dropwise and the resulting reaction mixture was then warmed up to room temperature before being heated at reflux overnight. Upon completion, the reaction mixture was cooled to room temperature, poured into saturated sodium acetate solution (375 mL) and stirred for 3 h. The organic layer was then extracted with DCM (x3), washed with water (x3) before being dried over magnesium sulfate, filtered and concentrated. The crude product was then purified by column chromatography (Hexanes: Ethyl Acetate 1:0 to 5:1) to obtain the pure product as a pale yellow solid in 67% yield (15.6 g).

^{1}H NMR (400 MHz, $CDCl_3$) δ 9.76 (s, 1H), 7.57 (d, *J* = 3.9 Hz, 1H), 7.27 (d, *J* = 4.2 Hz, 2H), 7.16 (d, *J* = 4.0 Hz, 1H), 7.05 – 6.90 (m, 1H). ^{13}C NMR (101 MHz, $CDCl_3$) δ 182.55, 147.16, 141.66, 137.32, 136.01, 128.34, 127.08, 126.14, 124.23. HRMS (ESI+): *m*/*z*. 194.99065 [$C_9H_7OS_2$ $(M+H)^+$, calcd 194.99328].

5-Bromo-2,2'-bithiophene-5'-carboxaldehyde (2)

1 (7.00 g, 36.2 mmol) was added in DMF (140 mL) and cooled to -20 °C. N-bromosuccinimide (6.77 g, 38.0 mmol) was then slowly added and the resulting reaction mixture was then stirred in the dark at room temperature for 24h. Upon completion, the reaction mixture was poured into iced water and stirred. The resulting precipitate was then filtered and dried. The crude product was then taken up in DCM, washed with water (x3), bring (x1) before being dried over magnesium sulfate, filtered through a short silica plug and concentrated to give the pure product as a pale-yellow solid in 81% yield (8.04 g).

^{1}H NMR (500 MHz, $CDCl_3$) δ 9.86 (s, 1H), 7.66 (d, J = 3.9 Hz, 1H), 7.18 (d, J = 3.9 Hz, 1H), 7.10 (d, J = 3.9 Hz, 1H), 7.03 (d, J = 3.9 Hz, 1H). ^{13}C NMR (126 MHz, $CDCl_3$) δ 182.48, 145.77, 141.95, 137.38, 137.18, 131.16, 126.17, 124.34, 114.13. HRMS (ESI+): *m*/*z*. 272.93912 [$C_9H_6OS_2Br$ $(M+H)^+$, calcd 272.90380].

5-(4-hydroxyphenyl)-2,2'-bithiophene-5'-carboxaldehyde (3)

2 (1.50 g, 5.49 mmol) was added with K_2CO_3 (1.80 g, 13.0 mmol), $Pd(PPh_3)_2Cl_2$ (135 mg, 0.19 mmol), 4-hydroxyphenylboronic acid (833 mg, 6.04 mmol) and placed under N_2. An N_2 sparged solution of DME (9 mL), EtOH (5 mL) and H_2O (7 mL) was then added to the reaction mixture, stirred and refluxed for 3.5 h. Upon completion, the reaction mixture was cooled and precipitated with minimal aqueous NaOH (1M). The precipitate was then filtered and washed with HCl (1M) to obtain the pure product as a yellow solid in 83% yield (1.31 g).

^{1}H NMR (400 MHz, DMSO) δ 9.87 (s, 1H), 7.98 (d, *J* = 3.9 Hz, 1H), 7.57 – 7.48 (m, 4H), 7.38 (d, *J* = 3.8 Hz, 1H), 6.83 (d, *J* = 8.5 Hz, 2H). ^{13}C NMR (101 MHz, DMSO) δ 183.68, 158.04, 145.95, 145.80, 140.78, 139.29, 132.55, 128.22, 127.02, 124.63, 123.89, 123.36, 116.01. HRMS (ESI+): *m*/*z*. 287.02683 [$C_{15}H_{11}O_2S_2$ $(M+H)^+$, calcd 287.01950].

NIAD-4

3 (200 mg, 0.710 mmol) was added with malononitrile (140mg, 2.12 mmol), NH_4OAc (213 mg, 2.77 mmol) and acetic acid (10 mL). The reaction mixture was then stirred and refluxed for 4 h. Upon completion of the reaction, the reaction mixture was cooled to room temperature and precipitated in water, filtered and dried. The crude product was then purified by column chromatography (Hexanes: Ethyl Acetate 1:0 to 2:1) to obtain the pure product as a red solid in 25% yield (58.2 mg).

^{1}H NMR (400 MHz, DMSO) δ 9.86 (s, 1H), 8.61 (s, 1H), 7.89 (d, *J* = 4.1 Hz, 1H), 7.66 (d, *J* = 3.9 Hz, 1H), 7.61 (d, *J* = 4.1 Hz, 1H), 7.56 (d, *J* = 8.6 Hz, 2H), 7.43 (d, *J* = 3.9 Hz, 1H), 6.83 (d, *J* = 8.6 Hz, 2H). ^{13}C NMR (101 MHz, DMSO) δ 158.25, 152.21, 148.19, 147.27, 142.68, 132.95, 131.92, 129.39, 127.20, 124.90, 123.82, 123.74, 116.04, 114.77, 114.07, 73.66. HRMS (ESI+): *m*/*z*. 335.03056 [$C_{18}H_{11}N_2OS_2$ $(M+H)^+$, calcd 335.03073].

NIAD-CNOET

3 (200 mg, 0.710 mmol) was added with ethyl cyanoacetate (803 mg, 7.10 mmol), 5 drops of piperidine and DCM (75 mL). The resulting reaction was stirred at room temperature for 48 h. Upon completion of the reaction, the organic layer was washed with water (x3), dried over magnesium sulfate, filtered and concentrated. The crude product was then purified by column chromatography (Hexanes: Ethyl Acetate 1:0 to 2:1) to obtain the pure product as a red solid in 30% yield (80.7 mg).

^{1}H NMR (400 MHz, DMSO) δ 9.84 (s, 1H), 8.54 (s, 1H), 8.03 (d, *J* = 4.0 Hz, 1H), 7.61 (d, *J* = 3.8 Hz, 1H), 7.58 – 7.55 (m, 3H), 7.42 (d, *J* = 3.9 Hz, 1H), 6.83 (d, *J* = 8.3 Hz 2H), 4.29 (q, *J* = 7.1 Hz, 2H), 1.30 (t, *J* = 7.1 Hz, 3H). ^{13}C NMR (101 MHz, DMSO) δ 162.33, 158.11, 146.93, 146.74, 146.53, 142.44, 133.33, 132.29, 128.63, 127.11, 124.64, 123.85, 123.64, 116.20, 116.02, 96.08, 62.03, 14.07. HRMS (ESI+): *m*/*z*. 382.05166 [$C_{20}H_{16}NO_3S_2$ $(M+H)^+$, calcd 382.05661].

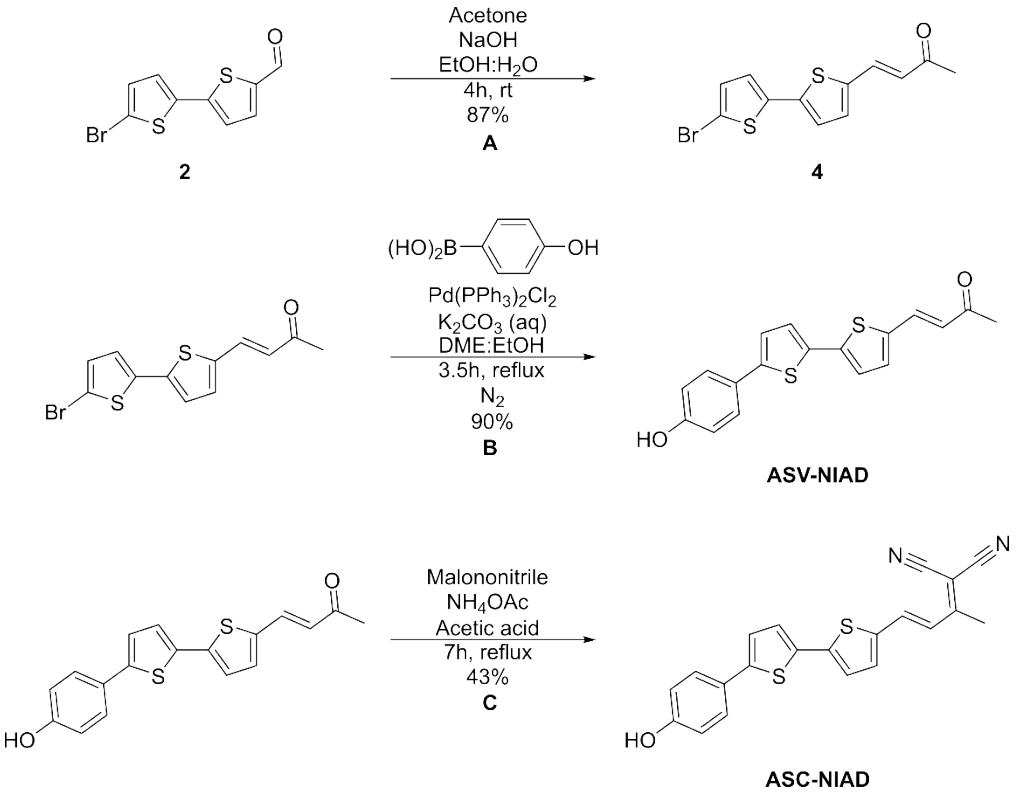

Scheme S2: Synthetic scheme for **ASV-NIAD** and **ASC-NIAD**. (A) Aldol condensation. (B) Palladium catalysed Suzuki coupling. (C) Knoevenagel condensation.

5-(3-oxo-1-butenyl)-5'-Bromo-2,2'-bithiophene (4)

2 (1.5 g, 5.50 mmol), acetone (15 mL) was added to EtOH (15 mL) and water (10 mL). NaOH (240 mg, 6.00 mmol) was then added and the reaction mixture was then stirred at room temperature for 4 h. Upon completion, the reaction mixture was precipitated in water, filtered and dried to give the pure product as a yellow solid in 87% yield (1.50 g).

^{1}H NMR (400 MHz, DMSO) δ 7.75 (d, *J* = 16.0 Hz, 1H), 7.55 – 7.47 (m, 1H), 7.37 – 7.36 (m. 1H), 7.27 – 7.26 (m, 2H), 6.46 (d, *J* = 16.0 Hz, 2H), 2.29 (s, 3H). ^{13}C NMR (101 MHz, DMSO) δ 197.23, 138.57, 138.22, 137.45, 135.35, 133.71, 131.92, 125.93, 125.85, 125.71, 111.72, 27.40. HRMS (ESI+): *m*/*z*. 394.93510 [$C_{12}H_{10}OS_2Br$ $(M+H)^+$, calcd 394.96227].

ASV-NIAD

4 (1.00 g, 3.19 mmol) was added with K_2CO_3 (926 g, 6.70 mmol), $Pd(PPh_3)_2Cl_2$ (78.5 mg, 0.11 mmol), 4-hydroxyphenylboronic acid (484 mg, 3.51 mmol) and placed under N_2. An N_2 sparged solution of DME (4.5 mL), EtOH (2.5 mL) and H_2O (3.5 mL) was then added to the reaction mixture, stirred and refluxed for 3.5 h. Upon completion, the reaction mixture was cooled and precipitated with minimal aqueous NaOH (1M). The precipitate was then filtered and washed with HCl (1M) to obtain the pure product as a yellow solid in 90% yield (931 mg).

^{1}H NMR (400 MHz, DMSO) δ 9.78 (s, 1H), 7.76 (d, *J* = 15.9 Hz, 1H), 7.53 – 7.47 (m, 3H), 7.42 – 7.30 (m, 3H), 6.86 – 6.78 (m, 2H), 6.43 (d, *J* = 16.0 Hz, 1H), 2.29 (s, 3H). ^{13}C NMR (101 MHz, DMSO) δ 197.17, 157.77, 144.43, 139.89, 137.63, 135.58, 134.01, 133.25, 126.85, 126.58, 125.30, 124.69, 124.12, 123.15, 115.97, 27.37. HRMS (ESI+): *m*/*z*. 327.05029 [$C_{18}H_{15}O_2S_2$ $(M+H)^+$, calcd 327.05080].

ASC-NIAD

ASV-NIAD (200 mg, 0.612 mmol) was added with malononitrile (121 mg, 1.84 mmol), NH_4OAc (184 mg, 2.38 mmol) and acetic acid (15 mL). The reaction mixture was then stirred and refluxed for 7 h. Upon completion of the reaction, the reaction mixture was cooled to room temperature and precipitated in water, filtered and dried. The crude product was then purified by column chromatography (Hexanes: Ethyl Acetate 5:1 to 1:2) to obtain the pure product as a dark red solid in 43% yield (98.7 mg).

^{1}H NMR (400 MHz, DMSO) δ 9.80 (s, 1H), 7.90 (d, *J* = 15.3 Hz, 2H), 7.57 – 7.53 (m, 4H), 7.41 – 7.36 (m, 2H), 6.89 – 6.81 (m, 3H), 2.41 (s, 3H). ^{13}C NMR (101 MHz, DMSO) δ 169.38, 157.92, 145.31, 142.17, 138.05, 138.01, 136.14, 132.97, 127.56, 126.94, 125.22, 124.03, 123.38, 121.19, 115.99, 114.01, 113.11, 79.37, 17.76. HRMS (ESI+): *m*/*z*. 375.05684 [$C_{21}H_{15}N_2O_2S_2$ $(M+H)^+$, calcd 375.06203].

2. X-ray Crystallography, DFT Calculations & Photophysical Studies

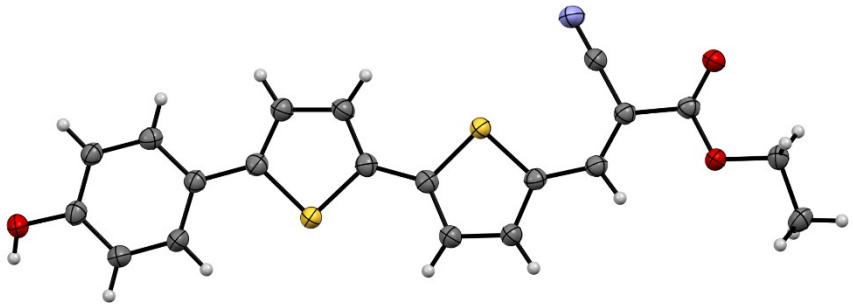

Figure S1: Crystal structure of NIAD-CNOET with R-factor of 4.92%.

Table S1: Crystal data and structure refinement for **NIAD-CNOET**.

CCDC code	2234385
Identification code	NIAD-CNOET
Empirical formula	$C_{20}H_{15}NO_3S_2$
Formula weight	381.45
Temperature/K	100.00(10)
Crystal system	triclinic
Space group	P-1
a/Å	6.7864(3)
b/Å	8.3598(5)
c/Å	15.6513(6)
α/°	92.948(4)
β/°	93.007(4)
γ/°	92.615(4)
Volume/Å^3	884.51(7)
Z	2
ρ_{calc}g/cm^3	1.432
μ/mm^{-1}	2.902
F(000)	396.0
Crystal size/mm^3	0.17 × 0.053 × 0.015
Radiation	Cu Kα (λ = 1.54184)
2Θ range for data collection/°	5.662 to 153.624
Index ranges	-6 ≤ h ≤ 8, -10 ≤ k ≤ 10, -19 ≤ l ≤ 19
Reflections collected	9692
Independent reflections	3614 [R_{int} = 0.0542, R_{sigma} = 0.0601]
Data/restraints/parameters	3614/0/240
Goodness-of-fit on F^2	1.065
Final R indexes [I>=2σ (I)]	R_1 = 0.0492, wR_2 = 0.1354
Final R indexes [all data]	R_1 = 0.0607, wR_2 = 0.1428
Largest diff. peak/hole / e Å^{-3}	0.47/-0.40

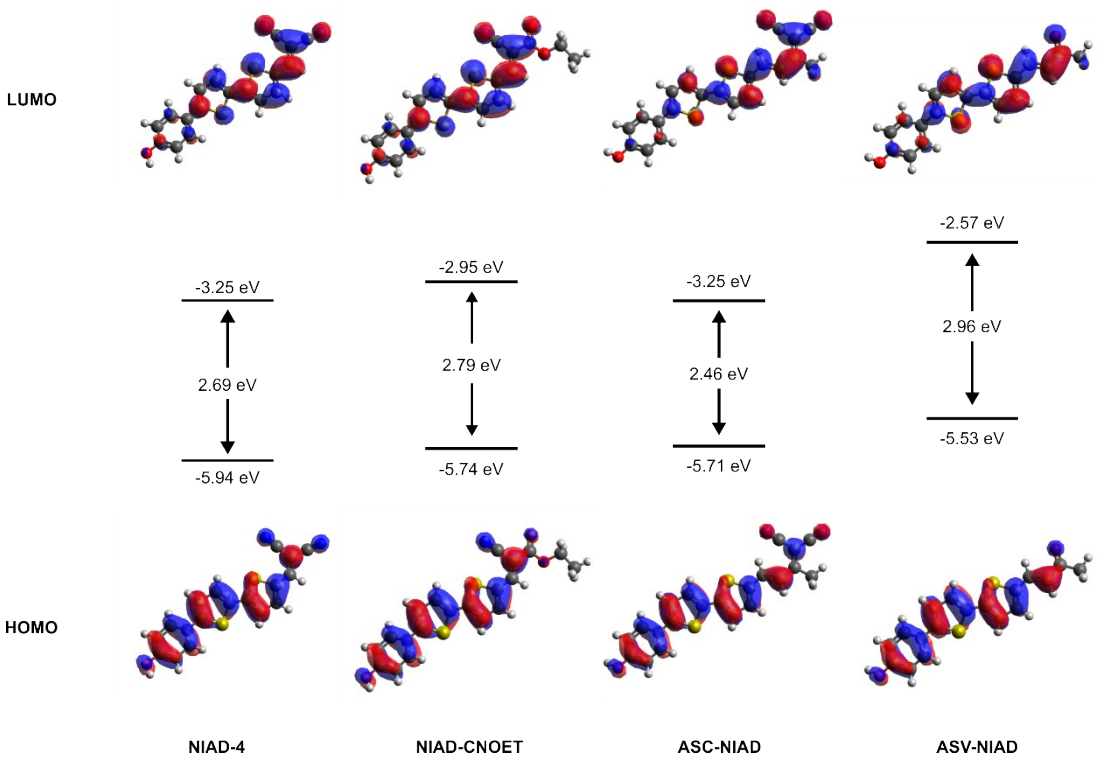

Figure S2: DFT calculations of HOMO and LUMO orbitals for NIAD-4, NIAD-CNOET, ASC-NIAD and ASV-NIAD. DFT calculations were carried out at the B3LYP/6-31+g(d,p) level. No negative frequencies for optimised structures were observed.

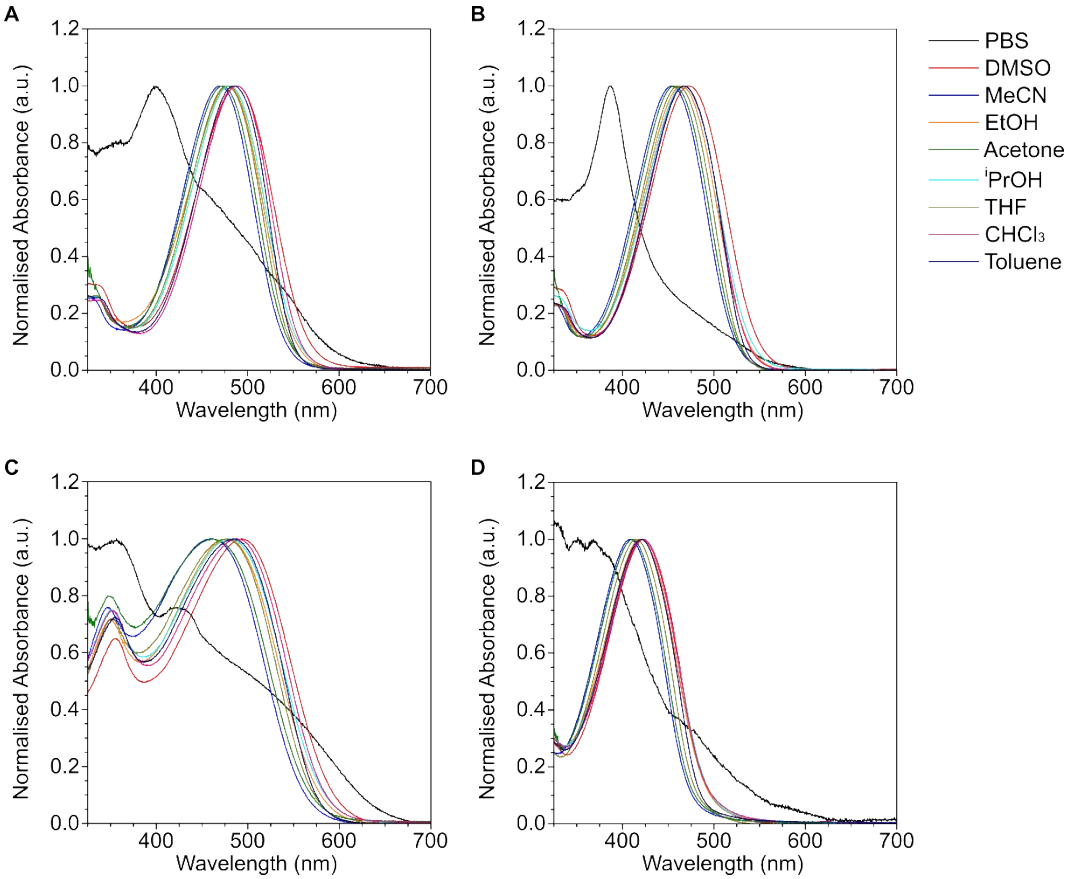

Figure S3: Absorbance spectra for NIAD-4 and derivatives in different solvents. (A) NIAD-4, (B) NIAD-CNOET, (C) ASC-NIAD, (D) ASV-NIAD. PBS was Na_2HPO_4 at 20 mM concentration. 10 μM dye concentration was used for all measurements.

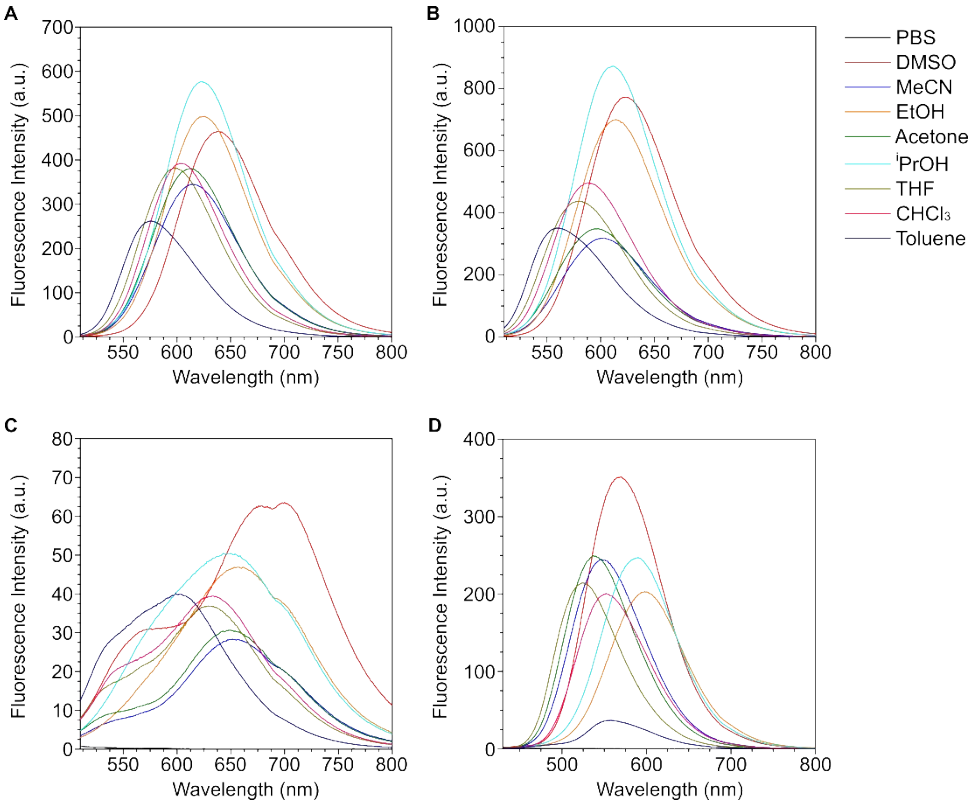

Figure S4: Fluorescence emission spectra for NIAD-4 and derivatives in different solvents. (A) NIAD-4, (B) NIAD-CNOET, (C) ASC-NIAD, (D) ASV-NIAD. PBS was Na_2HPO_4 at 20mM concentration. 10 µM dye concentration for all measurements. 405 nm wavelength was used for ASV-NIAD and 488 nm excitation was used for NIAD-4, NIAD-CNOET and ASC-NIAD.

3. Molecular Docking and Protein Aggregation

A

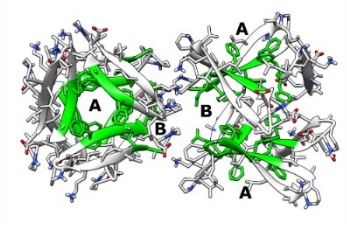

B

NIAD4	A	B
No. of Poses	500	-
Population (%)	100.0	-
Lowest Binding Energy	-11.36	-
Mean Binding Energy	-10.7	-
SD	0.36	-

NIAD-CNOET	A	B
No. of Poses	496	4
Population (%)	99.2	0.8
Lowest Binding Energy	-12.44	-9.08
Mean Binding Energy	-9.96	-8.98
SD	1.04	0.11

ASC-NIAD	A	B
No. of Poses	471	29
Population (%)	94.2	5.8
Lowest Binding Energy	-11.20	-9.85
Mean Binding Energy	-10.18	-9.61
SD	0.38	0.13

ASV-NIAD	A	B
No. of Poses	500	-
Population (%)	100.0	-
Lowest Binding Energy	-11.66	-
Mean Binding Energy	-11.23	-
SD	0.22	-

C

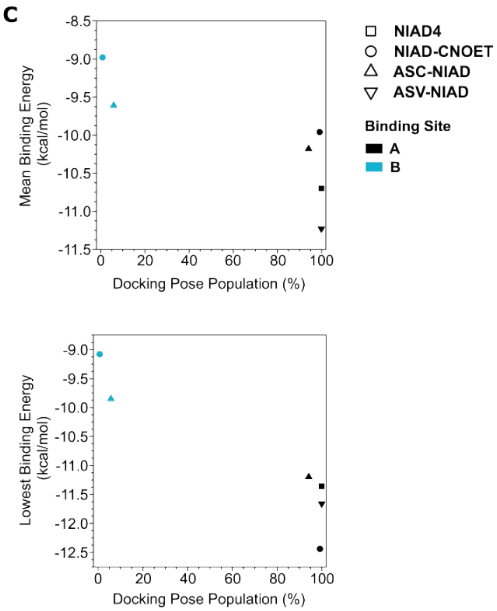

Figure S5: Analysis of docked poses on oligomer structure of Aβ with residues 17-36 (PDB: 4NTR). (A) Structure of Aβ 17-36 oligomers and docking sites of interest. (B,C) Summary of docking site populations, mean and lowest binding energies. SD refers to the standard deviation.

A

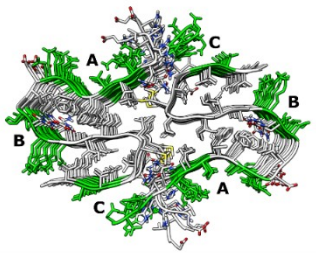

B

NIAD4	A	B	C
No. of Poses	2	1	496
Population (%)	0.4	0.2	99.2
Lowest Binding Energy	-7.50	-7.90	-8.95
Mean Binding Energy	-7.48	-7.90	-8.67
SD	0.04	-	0.24

NIAD-CNOET	A	B	C
No. of Poses	5	11	478
Population (%)	1.0	2.2	95.6
Lowest Binding Energy	-7.66	-8.47	-9.14
Mean Binding Energy	-7.26	-8.18	-8.53
SD	0.48	0.25	0.35

ASC-NIAD	A	B	C
No. of Poses	3	4	487
Population (%)	0.6	0.8	97.4
Lowest Binding Energy	-8.09	-8.91	-9.78
Mean Binding Energy	-7.69	-8.74	-9.29
SD	0.39	0.12	0.27

ASV-NIAD	A	B	C
No. of Poses	2	21	477
Population (%)	0.4	4.2	95.4
Lowest Binding Energy	-6.90	-8.19	-8.40
Mean Binding Energy	-6.70	-7.99	-7.96
SD	0.28	0.17	0.19

C

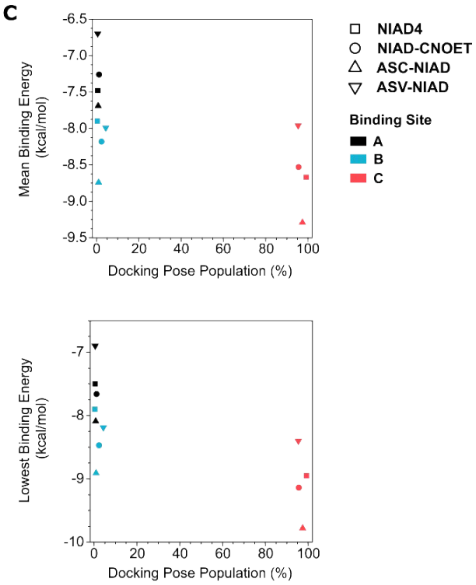

Figure S6: Analysis of docked poses of aβ 1-42 (PDB: 5KK3). (A) Structure of Aβ 1-42 and docking sites of interest. (B,C) Summary of mean and lowest binding energies. Summary of docking site populations, mean and lowest binding energies. SD refers to the standard deviation.

A

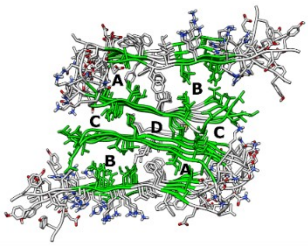

B

NIAD4	A	B	C	D
No. of Poses	49	351	14	86
Population (%)	9.8	70.2	2.8	17.2
Lowest Binding Energy	-10.22	-10.50	-9.48	-10.21
Mean Binding Energy	-9.84	-9.87	-9.42	-10.01
SD	0.32	0.32	0.04	0.2

NIAD-CNOET	A	B	C	D
No. of Poses	65	309	77	47
Population (%)	13.0	61.8	15.4	9.4
Lowest Binding Energy	-10.47	-10.97	-9.78	-9.79
Mean Binding Energy	-9.84	-9.69	-9.27	-9.49
SD	0.42	0.4	0.34	0.2

ASC-NIAD	A	B	C	D
No. of Poses	57	376	23	44
Population (%)	11.4	75.2	4.6	8.8
Lowest Binding Energy	-11.19	-11.30	-10.12	-10.45
Mean Binding Energy	-10.46	-10.69	-9.83	-10.14
SD	0.36	0.4	0.26	0.2

ASV-NIAD	A	B	C	D
No. of Poses	55	348	7	90
Population (%)	11.0	69.6	1.4	18.0
Lowest Binding Energy	-9.96	-9.70	-8.87	-10.34
Mean Binding Energy	-9.25	-9.17	-8.73	-9.21
SD	0.34	0.18	0.16	0.45

C

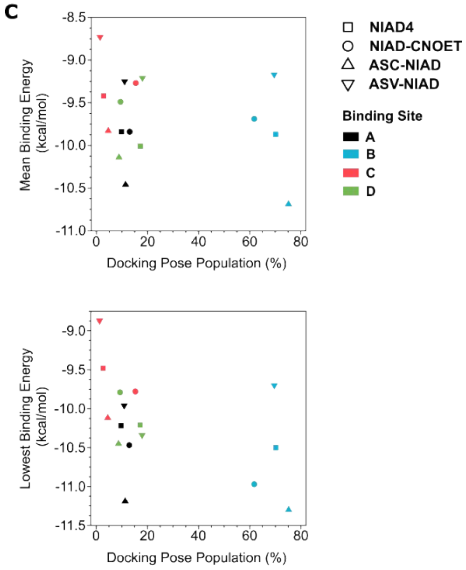

Figure S7: Analysis of docked poses of Aβ 1-40 (PDB: 2LMO). (A) Structure of Aβ 1-40 and docking sites of interest. (B,C) Summary of docking site populations, mean and lowest binding energies. SD refers to the standard deviation.

A

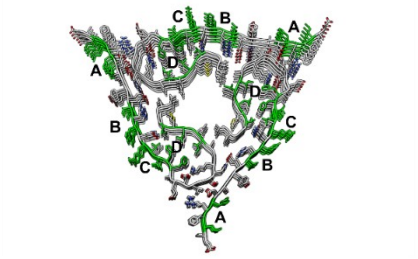

B

NIAD4	A	B	C	D
No. of Poses	491	4	2	3
Population (%)	98.2	0.8	0.4	0.6
Lowest Binding Energy	-8.89	-7.81	-7.85	-7.37
Mean Binding Energy	-8.48	-7.78	-7.80	-7.05
SD	0.19	0.05	0.07	0.33

NIAD-CNOET	A	B	C	D
No. of Poses	474	15	2	8
Population (%)	94.8	3.0	0.4	1.6
Lowest Binding Energy	-9.29	-7.78	-8.18	-7.72
Mean Binding Energy	-8.61	-7.39	-7.78	-7.04
SD	0.35	0.23	0.57	0.46

ASC-NIAD	A	B	C	D
No. of Poses	481	13	-	4
Population (%)	96.2	2.6	-	0.8
Lowest Binding Energy	-10.25	-8.83	-	-7.85
Mean Binding Energy	-9.62	-8.31	-	-7.81
SD	0.32	0.37	-	0.05

ASV-NIAD	A	B	C	D
No. of Poses	487	6	1	6
Population (%)	97.4	1.2	0.2	1.2
Lowest Binding Energy	-8.79	-7.65	-7.59	-6.94
Mean Binding Energy	-8.34	-7.41	-7.59	-6.86
SD	0.25	0.26	-	0.07

C

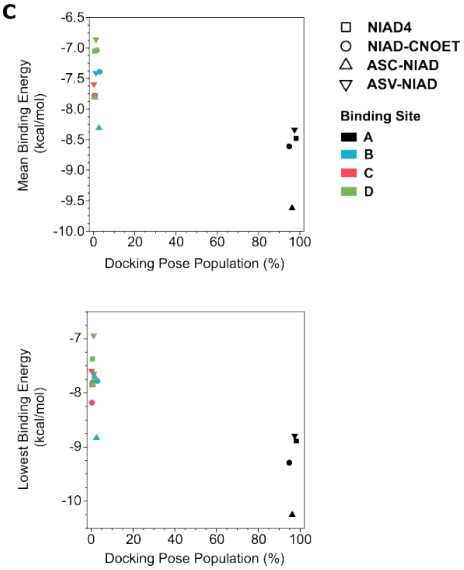

Figure S8: Analysis of docked poses of Aβ 1-40 (PDB: 24MJ). (A) Structure of Aβ 1-40 and docking sites of interest. (B,C) Summary of docking site populations, mean and lowest binding energies. SD refers to the standard deviation.

A

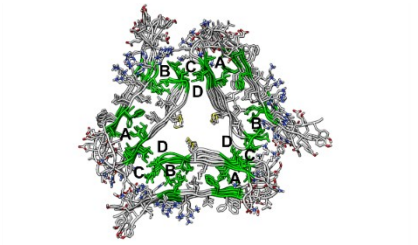

B

NIAD4	A	B	C	D
No. of Poses	494	6	-	-
Population (%)	98.8	1.2	-	-
Lowest Binding Energy	-11.18	-11.49	-	-
Mean Binding Energy	-10.81	-10.53	-	-
SD	0.26	0.88	-	-

NIAD-CNOET	A	B	C	D
No. of Poses	477	19	-	4
Population (%)	95.4	3.8	-	0.8
Lowest Binding Energy	-11.77	-10.74	-	-9.7
Mean Binding Energy	-10.80	-9.52	-	-9.61
SD	0.43	0.65	-	0.1

ASC-NIAD	A	B	C	D
No. of Poses	483	15	1	1
Population (%)	96.6	3.0	0.2	0.2
Lowest Binding Energy	-12.23	-10.92	-10.49	-10.25
Mean Binding Energy	-11.64	-10.49	-10.49	-10.25
SD	0.33	0.4	-	-

ASV-NIAD	A	B	C	D
No. of Poses	498	2	-	-
Population (%)	99.6	0.4	-	-
Lowest Binding Energy	-10.82	-10.63	-	-
Mean Binding Energy	-10.40	-10.60	-	-
SD	0.32	0.05	-	-

C

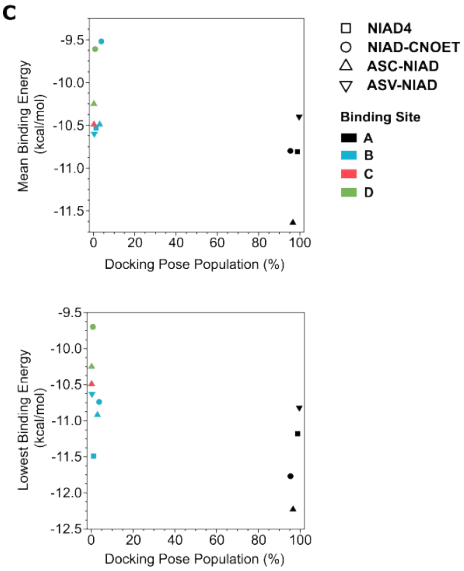

Figure S9: Analysis of docked poses of Aβ 1-40 (PDB: 2MLQ). (A) Structure of Aβ 1-40 and docking sites of interest. (B,C) Summary of docking site populations, mean and lowest binding energies. SD refers to the standard deviation.

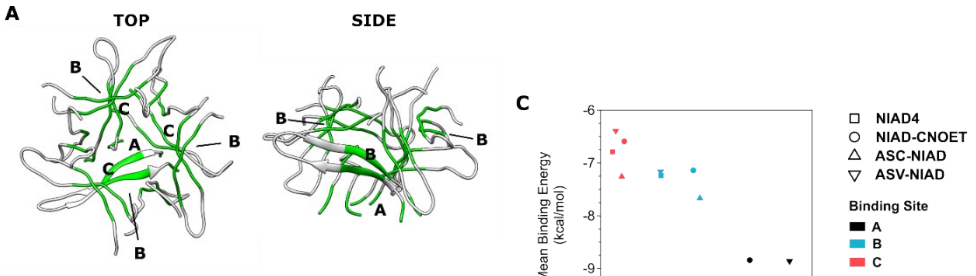

B

NIAD4	A	B	C
No. of Poses	369	110	14
Population (%)	73.8	22.0	2.8
Lowest Binding Energy	-9.64	-7.97	-7.2
Mean Binding Energy	-9.36	-7.24	-6.79
SD	0.45	0.26	0.17

NIAD-CNOET	A	B	C
No. of Poses	286	174	37
Population (%)	57.2	34.8	7.4
Lowest Binding Energy	-9.58	-8.60	-8.89
Mean Binding Energy	-8.84	-7.14	-6.59
SD	0.54	0.51	0.53

ASC-NIAD	A	B	C
No. of Poses	281	187	32
Population (%)	56.2	37.4	6.4
Lowest Binding Energy	-9.90	-8.71	-7.66
Mean Binding Energy	-9.47	-7.67	-7.26
SD	0.39	0.36	0.26

ASV-NIAD	A	B	C
No. of Poses	365	109	20
Population (%)	73.0	21.8	4
Lowest Binding Energy	-9.18	-7.71	-6.82
Mean Binding Energy	-8.86	-7.16	-6.39
SD	0.42	0.4	0.13

Figure S10: Analysis of docked poses of α-syn. (A) Structure of α-syn and docking sites of interest (PDB: 5F1T). (B,C) Summary of docking site populations, mean and lowest binding energies. SD refers to the standard deviation. For clarity, only oligomer backbone is shown.

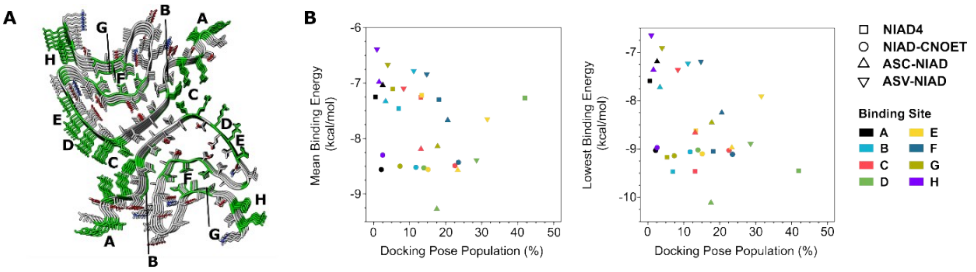

C

NIAD4	A	B	C	D	E	F	G	H
No. of Poses	3	35	66	210	67	91	27	-
Population (%)	0.6	7.0	13.2	42.0	13.4	18.2	5.4	-
Lowest Binding Energy	-7.59	-9.47	-9.46	-9.45	-8.62	-9.05	-9.17	-
Mean Binding Energy	-7.25	-7.46	-7.26	-7.27	-7.22	-7.30	-7.11	-
SD	0.35	0.69	0.57	0.64	0.57	0.58	0.69	-

NIAD-CNOET	A	B	C	D	E	F	G	H
No. of Poses	11	59	113	70	76	118	37	13
Population (%)	2.2	11.8	22.6	14.0	15.2	23.6	7.4	2.6
Lowest Binding Energy	-9.03	-9.06	-9.03	-9.02	-9.10	-9.11	-9.14	-8.97
Mean Binding Energy	-8.56	-8.52	-8.49	-8.53	-8.56	-8.43	-8.50	-8.30
SD	0.35	0.47	0.41	0.33	0.34	0.43	0.41	0.77

ASC-NIAD	A	B	C	D	E	F	G	H
No. of Poses	13	17	66	88	117	103	89	8
Population (%)	2.6	3.4	13.2	17.6	23.4	20.6	17.8	1.6
Lowest Binding Energy	-7.19	-7.72	-8.66	-10.11	-8.97	-8.25	-8.45	-7.36
Mean Binding Energy	-7.04	-7.33	-8.19	-9.27	-8.57	-7.67	-8.14	-6.98
SD	0.11	0.23	0.33	0.61	0.29	0.32	0.34	0.26

ASV-NIAD	A	B	C	D	E	F	G	H
No. of Poses	-	56	42	143	158	74	20	5
Population (%)	-	11.2	8.4	28.6	31.6	14.8	4.0	1.0
Lowest Binding Energy	-	-7.23	-7.36	-8.89	-7.91	-7.19	-6.91	-6.65
Mean Binding Energy	-	-6.78	-7.10	-8.39	-7.65	-6.84	-6.67	-6.39
SD	-	0.30	0.14	0.52	0.16	0.26	0.16	0.24

Figure S11: Analysis of docked poses of α-syn. (A) Structure of α-syn and docking sites of interest (PDB: 6CU7). (B,C) Summary of docking site populations, mean and lowest binding energies. SD refers to the standard deviation.

A

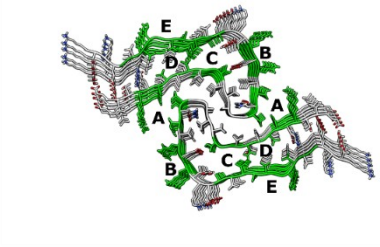

B

NIAD4	A	B	C	D	E
No. of Poses	-	499	-	-	-
Population (%)	-	99.8	-	-	-
Lowest Binding Energy	-	-8.90	-	-	-
Mean Binding Energy	-	-8.63	-	-	-
SD	-	0.13	-	-	-

NIAD-CNOET	A	B	C	D	E
No. of Poses	3	480	3	12	2
Population (%)	0.6	96.0	0.6	2.4	0.4
Lowest Binding Energy	-7.62	-9.35	-7.96	-7.53	-7.94
Mean Binding Energy	-7.54	-8.82	-7.91	-7.25	-7.77
SD	0.09	0.27	0.07	0.21	0.24

ASC-NIAD	A	B	C	D	E
No. of Poses	2	476	8	14	-
Population (%)	0.4	95.2	1.6	2.8	-
Lowest Binding Energy	-8.52	-9.97	-8.94	-8.60	-
Mean Binding Energy	-8.32	-9.57	-8.83	-8.21	-
SD	0.28	0.22	0.15	0.29	-

ASV-NIAD	A	B	C	D	E
No. of Poses	-	486	1	13	-
Population (%)	-	97.2	0.2	2.6	-
Lowest Binding Energy	-	-8.99	-7.87	-7.51	-
Mean Binding Energy	-	-8.58	-7.87	-7.40	-
SD	-	0.17	-	0.06	-

C

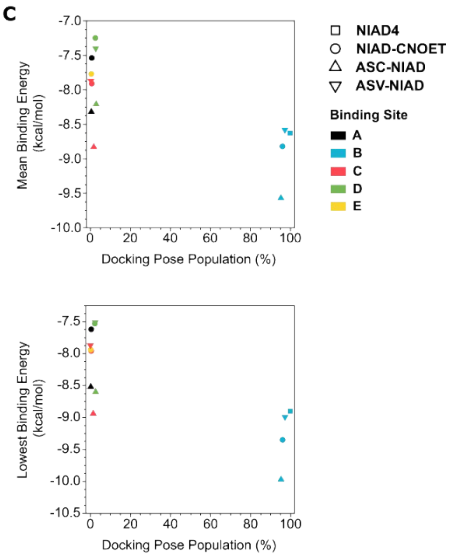

Figure S12: Analysis of docked poses of α-syn. (A) Structure of α-syn and docking sites of interest (PDB: 6CU8). (B,C) Summary of docking site populations, mean and lowest binding energies. SD refers to the standard deviation.

A

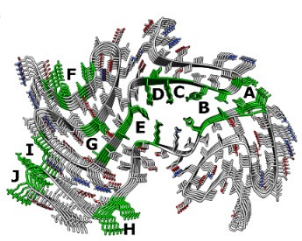

B

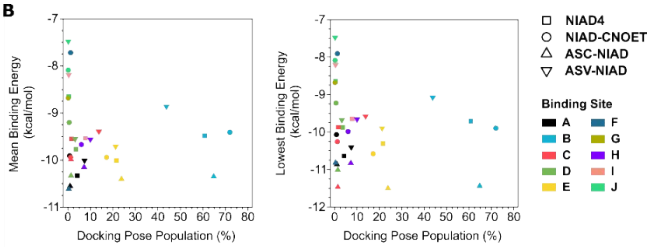

C

NIAD4	A	B	C	D	E	F	G	H	I	J
No. of Poses	21	304	8	18	108	-	-	-	39	2
Population (%)	4.2	60.8	1.6	3.6	21.6	-	-	-	7.8	0.4
Lowest Binding Energy	-10.64	-9.71	-9.87	-9.88	-10.31	-	-	-	-9.65	-8.65
Mean Binding Energy	-10.33	-9.48	-9.55	-9.77	-10.01	-	-	-	-9.54	-8.65
SD	0.30	0.14	0.34	0.13	0.25	-	-	-	0.14	0.01

NIAD-CNOET	A	B	C	D	E	F	G	H	I	J
No. of Poses	4	360	6	3	86	6	1	30	-	1
Population (%)	0.8	72.0	1.2	0.6	17.2	1.2	0.2	6.0	-	0.2
Lowest Binding Energy	-10.07	-9.90	-10.26	-9.23	-10.58	-7.91	-8.68	-9.99	-	-8.09
Mean Binding Energy	-9.91	-9.41	-9.94	-9.20	-9.94	-7.72	-8.68	-9.67	-	-8.09
SD	0.16	0.20	0.34	0.05	0.50	0.13	-	0.25	-	-

ASC-NIAD	A	B	C	D	E	F	G	H	I	J
No. of Poses	5	324	7	7	119	2	-	36	-	-
Population (%)	1.0	64.8	1.4	1.4	23.8	0.4	-	7.2	-	-
Lowest Binding Energy	-10.86	-11.44	-11.47	-11.01	-11.50	-10.82	-	-10.83	-	-
Mean Binding Energy	-10.55	-10.35	-9.99	-10.33	-10.40	-10.61	-	-10.15	-	-
SD	0.25	0.49	0.83	0.47	0.47	0.30	-	0.41	-	-

ASV-NIAD	A	B	C	D	E	F	G	H	I	J
No. of Poses	37	219	69	16	106	-	-	50	2	1
Population (%)	7.4	43.8	13.8	3.2	21.2	-	-	10.0	0.4	0.2
Lowest Binding Energy	-10.41	-9.08	-9.58	-9.68	-9.90	-	-	-9.66	-8.21	-7.48
Mean Binding Energy	-10.01	-8.86	-9.39	-9.55	-9.71	-	-	-9.56	-8.19	-7.48
SD	0.29	0.10	0.11	0.07	0.13	-	-	0.13	0.03	-

Figure S13: Analysis of docked poses of α-syn from MSA patient structure type 1 (PDB: 6XYO). (A) Structure of α-syn and docking sites of interest. (B,C) Summary of docking site populations, mean and lowest binding energies. SD refers to the standard deviation.

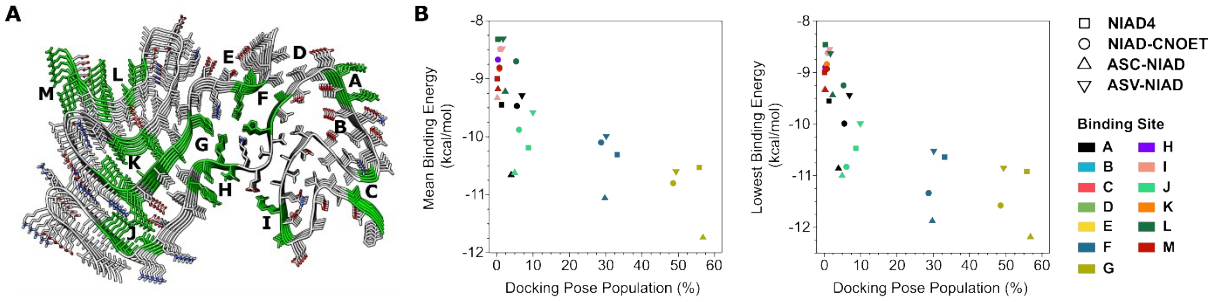

C

NIAD4	A	B	C	D	E	F	G	H	I	J	K	L	M
No. of Poses	7	-	-	-	-	166	279	-	-	44	-	2	1
Population (%)	1.4	-	-	-	-	33.2	55.8	-	-	8.8	-	0.4	0.2
Lowest Binding Energy	-9.55	-	-	-	-	-10.64	-10.92	-	-	-10.47	-	-8.46	-9.00
Mean Binding Energy	-9.45	-	-	-	-	-10.31	-10.53	-	-	-10.19	-	-8.32	-9.00
SD	0.15	-	-	-	-	0.25	0.26	-	-	0.30	-	0.20	-

NIAD-CNOET	A	B	C	D	E	F	G	H	I	J	K	L	M
No. of Poses	28	-	-	-	-	144	243	2	5	31	4	27	4
Population (%)	5.6	-	-	-	-	28.8	48.6	0.4	1.0	6.2	0.8	5.4	0.8
Lowest Binding Energy	-9.99	-	-	-	-	-11.34	-11.58	-8.90	-8.62	-10.83	-8.84	-9.25	-8.93
Mean Binding Energy	-9.47	-	-	-	-	-10.10	-10.80	-8.67	-8.49	-9.88	-8.83	-8.70	-8.81
SD	0.32	-	-	-	-	0.50	0.55	0.33	0.08	0.51	0.01	0.42	0.13

ASC-NIAD	A	B	C	D	E	F	G	H	I	J	K	L	M
No. of Poses	20	-	-	-	-	149	284	-	1	25	-	12	2
Population (%)	4.0	-	-	-	-	29.8	56.8	-	0.2	5.0	-	2.4	0.4
Lowest Binding Energy	-10.86	-	-	-	-	-11.88	-12.19	-	-9.33	-11.00	-	-9.44	-9.34
Mean Binding Energy	-10.66	-	-	-	-	-11.06	-11.74	-	-9.33	-10.62	-	-9.22	-9.18
SD	0.16	-	-	-	-	0.62	0.29	-	-	0.26	-	0.15	0.23

ASV-NIAD	A	B	C	D	E	F	G	H	I	J	K	L	M
No. of Poses	35	-	-	-	-	151	247	-	8	50	-	9	-
Population (%)	7.0	-	-	-	-	30.2	49.4	-	1.6	10.0	-	1.8	-
Lowest Binding Energy	-9.44	-	-	-	-	-10.52	-10.85	-	-8.55	-9.99	-	-8.63	-
Mean Binding Energy	-9.29	-	-	-	-	-9.99	-10.60	-	-8.48	-9.58	-	-8.31	-
SD	0.18	-	-	-	-	0.40	0.28	-	0.10	0.25	-	0.20	-

Figure S14: Analysis of docked poses of α-syn from MSA patient structure type 2-A (PDB: 6XYP). (A) Structure of α-syn and docking sites of interest. (B,C) Summary of docking site populations, mean and lowest binding energies. SD refers to the standard deviation.

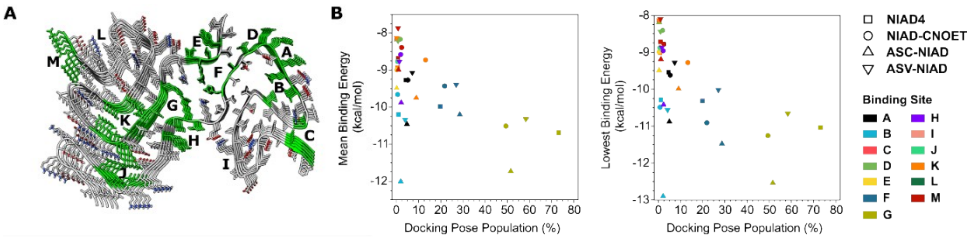

C

NIAD4	A	B	C	D	E	F	G	H	I	J	K	L	M
No. of Poses	22	5	-	-	-	99	366	-	-	-	3	-	4
Population (%)	4.4	1.0	-	-	-	19.8	73.2	-	-	-	0.6	-	0.8
Lowest Binding Energy	-9.54	-10.29	-	-	-	-10.32	-11.04	-	-	-	-9.02	-	-8.72
Mean Binding Energy	-9.27	-10.2	-	-	-	-9.98	-10.69	-	-	-	-8.93	-	-8.68
SD	0.23	0.07	-	-	-	0.26	0.26	-	-	-	0.14	-	0.04

NIAD-CNOET	A	B	C	D	E	F	G	H	I	J	K	L	M
No. of Poses	26	3	1	9	1	109	247	10	-	3	66	-	12
Population (%)	5.2	0.6	0.2	1.8	0.2	21.8	49.4	2.0	-	0.6	13.2	-	2.4
Lowest Binding Energy	-9.62	-10.49	-8.17	-8.41	-8.99	-10.91	-11.26	-8.96	-	-8.88	-9.28	-	-8.78
Mean Binding Energy	-9.27	-9.66	-8.17	-8.17	-8.99	-9.43	-10.51	-8.58	-	-8.77	-8.73	-	-8.39
SD	0.22	1.3	-	0.17	-	0.61	0.57	0.32	-	0.09	0.32	-	0.24

ASC-NIAD	A	B	C	D	E	F	G	H	I	J	K	L	M
No. of Poses	24	10	-	1	1	143	258	11	-	-	45	-	5
Population (%)	4.8	2.0	-	0.2	0.2	28.6	51.6	2.2	-	-	9	-	1
Lowest Binding Energy	-10.88	-12.90	-	-8.19	-9.49	-11.48	-12.54	-10.42	-	-	-9.99	-	-9.19
Mean Binding Energy	-10.46	-12.01	-	-8.19	-9.49	-10.2	-11.73	-9.88	-	-	-9.75	-	-8.99
SD	0.39	0.89	-	-	-	0.82	0.62	0.35	-	-	0.3	-	0.26

ASV-NIAD	A	B	C	D	E	F	G	H	I	J	K	L	M
No. of Poses	36	20	-	4	-	135	292	7	-	-	1	-	4
Population (%)	7.2	4.0	-	0.8	-	27.0	58.4	1.4	-	-	0.2	-	0.8
Lowest Binding Energy	-9.28	-10.56	-	-8.44	-	-10.02	-10.66	-8.87	-	-	-8.13	-	-8.1
Mean Binding Energy	-9.07	-10.34	-	-8.21	-	-9.39	-10.32	-8.77	-	-	-8.13	-	-7.87
SD	0.08	0.19	-	0.33	-	0.41	0.25	0.05	-	-	-	-	0.26

Figure S15: Analysis of docked poses of α-syn from MSA patient structure type 2-B (PDB: 6XYQ). (A) Structure of αSyn and docking sites of interest. (B,C) Summary of docking site populations, mean and lowest binding energies. SD refers to the standard deviation.

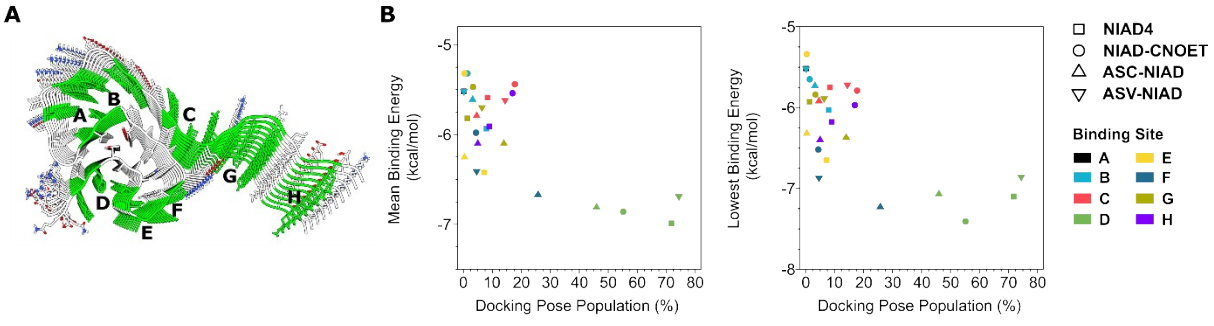

C

NIAD4	A	B	C	D	E	F	G	H
No. of Poses	1	8	42	359	36	-	7	45
Population (%)	0.2	8.0	8.4	71.8	7.2	-	1.4	9.0
Lowest Binding Energy	-5.52	-6.03	-5.75	-7.10	-6.65	-	-5.93	-6.18
Mean Binding Energy	-5.52	-5.93	-5.59	-6.99	-6.42	-	-5.82	-5.91
SD	0.00	0.08	0.08	0.08	0.17	-	0.08	0.13

NIAD-CNOET	A	B	C	D	E	F	G	H
No. of Poses	-	7	89	276	2	22	17	85
Population (%)	-	1.4	17.8	55.2	0.4	4.4	3.4	17.0
Lowest Binding Energy	-	-5.65	-5.79	-7.41	-5.34	-6.52	-5.84	-5.97
Mean Binding Energy	-	-5.32	-5.44	-6.86	-5.32	-5.98	-5.47	-5.54
SD	-	0.19	0.18	0.31	0.02	0.35	0.23	0.16

ASC-NIAD	A	B	C	D	E	F	G	H
No. of Poses	-	16	23	230	2	129	70	25
Population (%)	-	3.2	4.6	46.0	0.4	25.8	14.0	5.0
Lowest Binding Energy	-	-5.73	-5.92	-7.07	-6.32	-7.23	-6.37	-6.40
Mean Binding Energy	-	-5.61	-5.79	-6.81	-6.25	-6.67	-6.10	-6.10
SD	-	0.07	0.09	0.16	0.08	0.28	0.14	0.19

ASV-NIAD	A	B	C	D	E	F	G	H
No. of Poses	-	1	72	372	-	23	32	-
Population (%)	-	0.2	14.4	74.4	-	4.6	6.4	-
Lowest Binding Energy	-	-5.52	-5.72	-6.86	-	-6.87	-5.89	-
Mean Binding Energy	-	-5.52	-5.62	-6.69	-	-6.41	-5.70	-
SD	-	0.00	0.08	0.13	-	0.21	0.11	-

Figure S16: Analysis of docked poses of α-syn (PDB: 2N0A). (A) Structure of α-syn and docking sites of interest. (B,C) Summary of docking site populations, mean and lowest binding energies. SD refers to the standard deviation. Note, modelling was only carried out on amino acid sequence ranging from G31 to Q99.

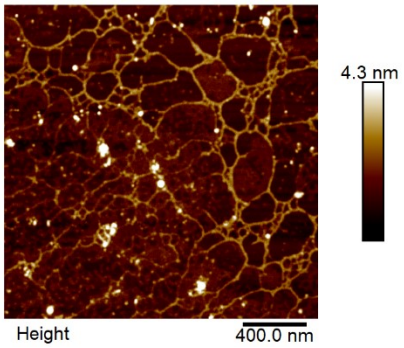

Figure S17: Representative atomic force microscopy (AFM) image confirming the formation of α-Synuclein preformed fibrils.

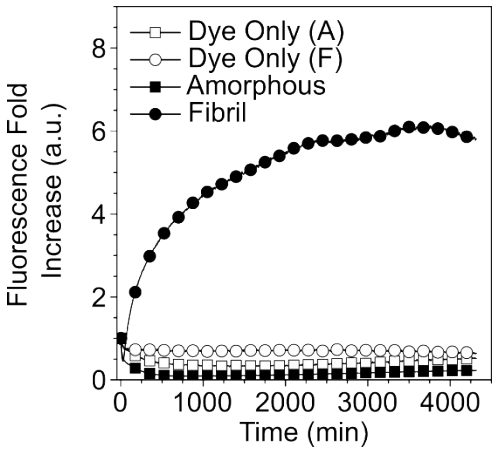

Figure S18: Fluorescence kinetics of ovalbumin with ThT. The excitation and emission filters were 440/10 and 485/20 respectively. 10 µM dye and 1 mg/mL ovalbumin concentration was used for all conditions. n = 4 biological replicates. Note: Dye only (A) and Dye Only (F) refer to the corresponding aggregation buffer conditions without ovalbumin.

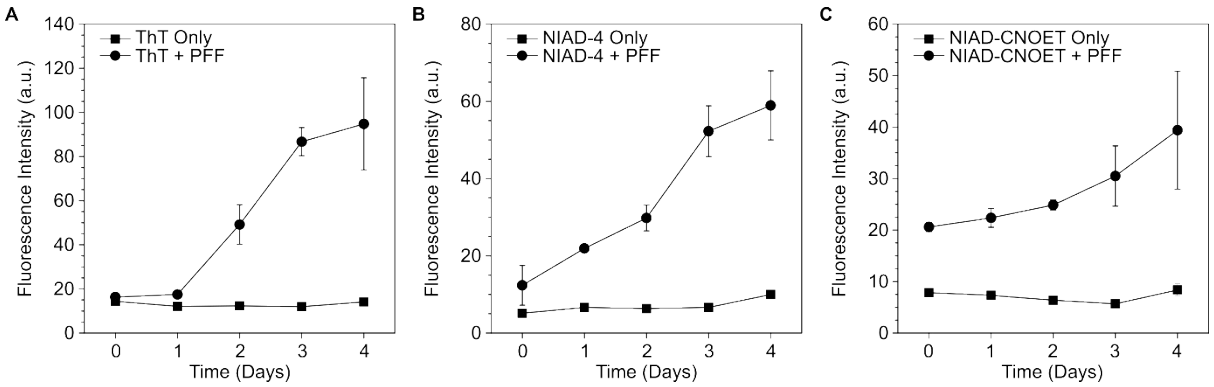

Figure S19: Discontinuous fluorescence kinetics of α-Synuclein preformed fibrils (α-Syn PFF). (A) ThT, (B) NIAD4, (C) NIAD-CNOET. For ThT the excitation and emission filters were set at 444/15 and 488/20 nm. For NIAD4 and NIAD-CNOET the excitation and emission filter were set at 488/10 and 575/20 nm respectively. 50 µM of dye and 140 µM of α-syn PFF was used for the respective conditions. n = 3 technical replicates.

4. Cell Viability, Confocal Laser Scanning Microscopy and Flow Cytometry

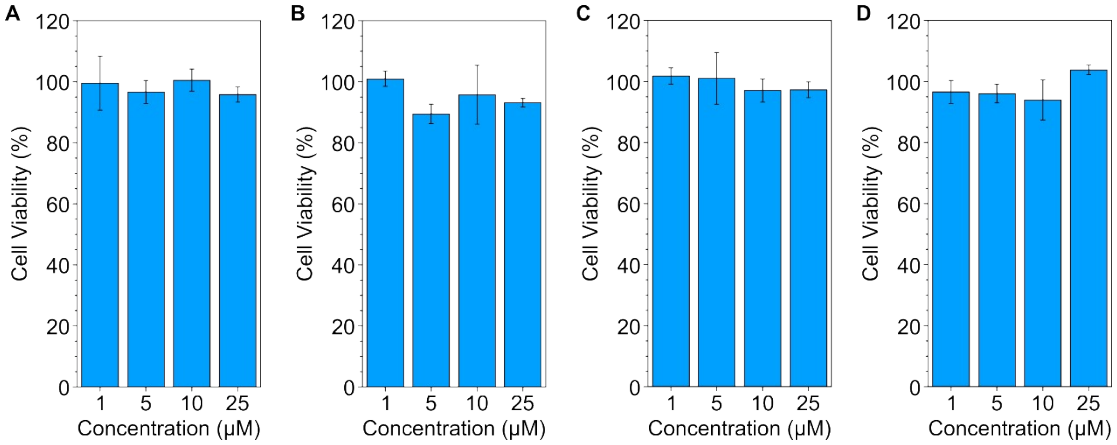

Figure S20: Cell viability experiments. (A) NIAD-4. (B) NIAD-CNOET. (C) ASC-NIAD. (D) ASV-NIAD. Cells were treated for 1 h with respective dyes and concentrations. Resazurin (alamarBlue™) cell viability assay was recorded on a plate reader. n = 4 biological replicates; mean ± s.d.

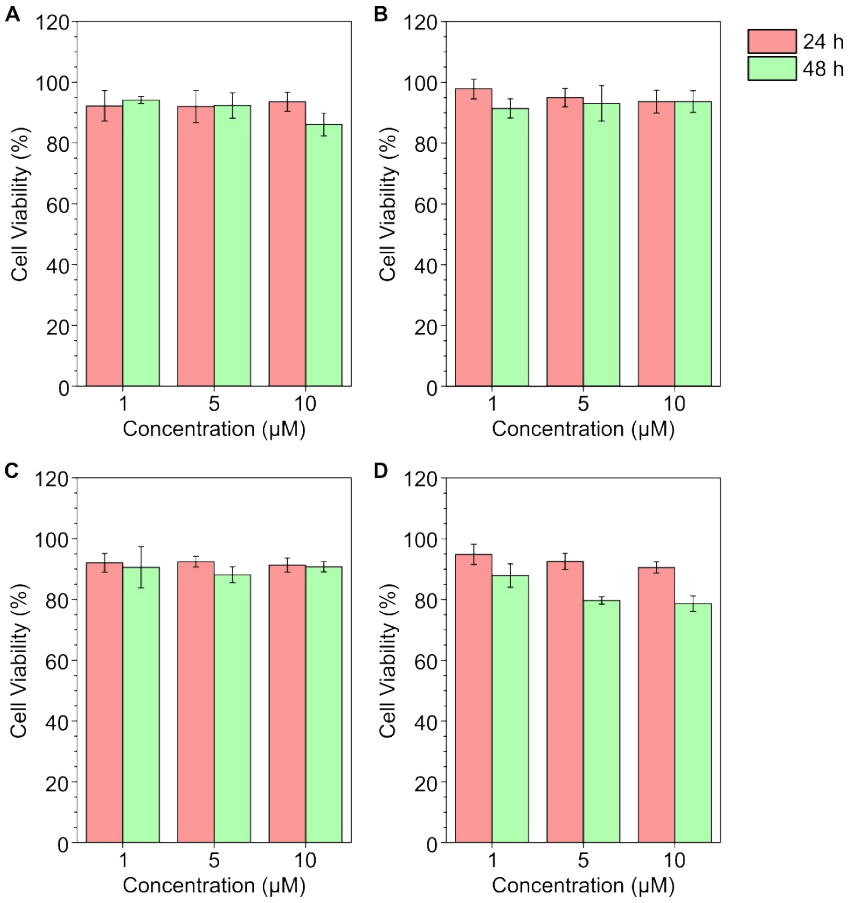

Figure S21: Cell viability experiments. (A) NIAD-4. (B) NIAD-CNOET. (C) ASC-NIAD. (D) ASV-NIAD. Cells were treated for 24 and 48 h with respective dyes and concentrations. Resazurin (alamarBlue™) cell viability assay was recorded on a plate reader. n = 4 biological replicates; mean ± s.d.

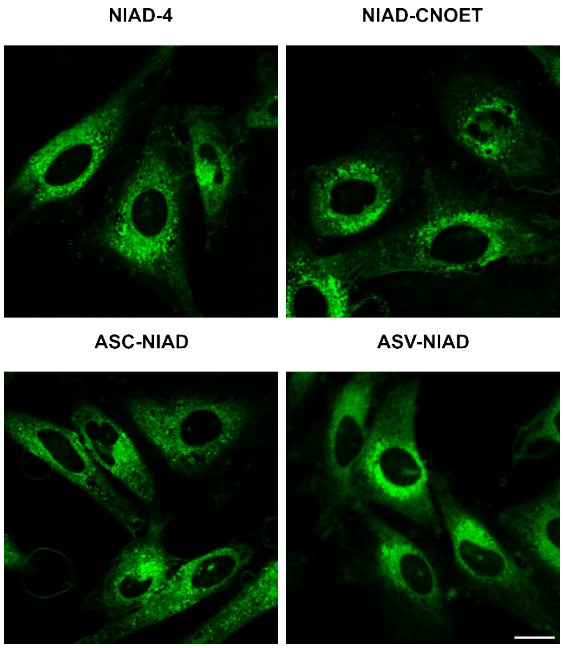

Figure S22: Confocal images of dye stained HeLa cells followed by fixation. Cells were stained with 1 μM of dye. Scale Bar, 20μm. For NIAD-4, NIAD-CNOET and ASC-NIAD, (excitation: 488 nm; emission: 550 – 650 nm), ASV-NIAD (excitation: 405 nm; emission 550 – 650 nm).

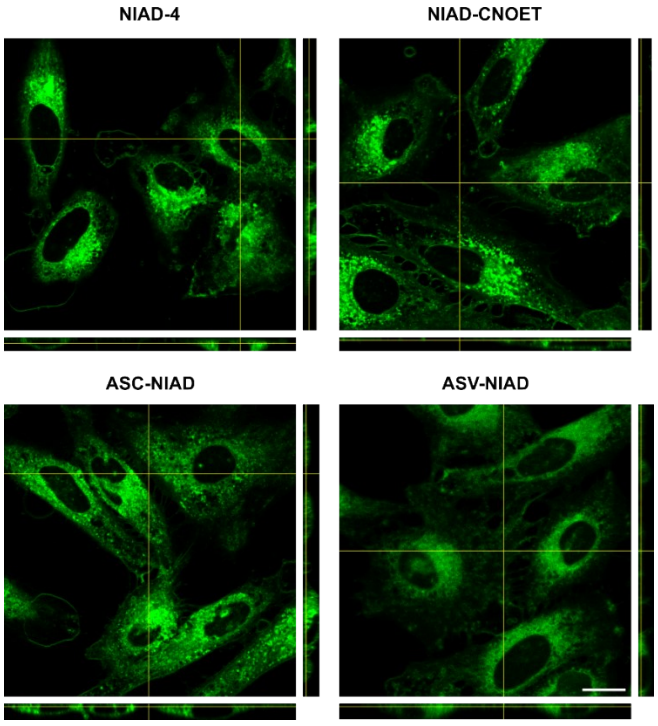

Figure S23: Z-stack image for confirmation of dye localisation in stained HeLa cells with fixation. Cells were stained with 1 μM of dye. Scale Bar, 20 μm. For NIAD-4, NIAD-CNOET and ASC-NIAD, (excitation: 488 nm; emission: 550 – 650 nm), ASV-NIAD (excitation: 405 nm; emission 550 – 650 nm).

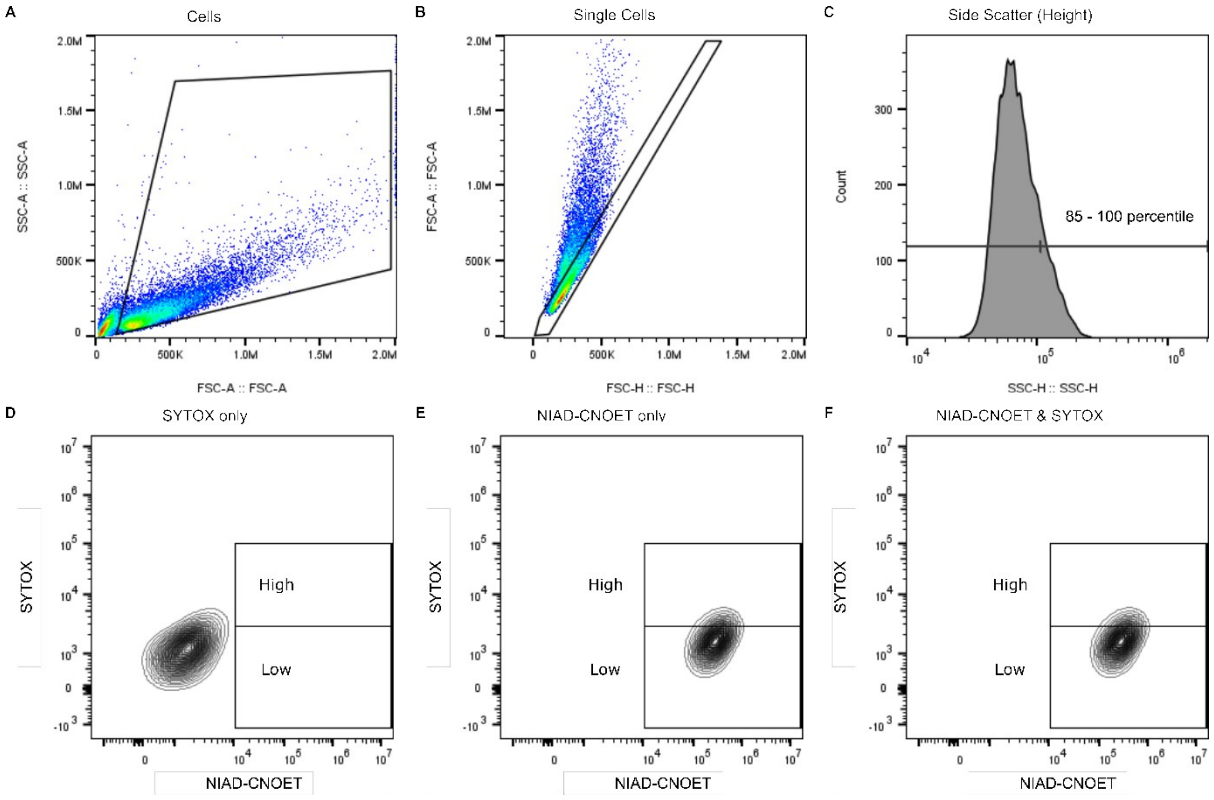

Figure S24: General flow cytometry gating strategy and control conditions – example shown for NIAD-CNOET and corresponding conditions. (A) Cells were first gated followed by (B) single cells. (C) Cells were then gated based on their side scatter (height) at 0 – 85 and 85 – 100 percentiles. (D – F) The cells gated by their side scatter profile was then counted by their intensity, with focus on the 85 – 100 percentile of side scatter profiles in the high gate population count.

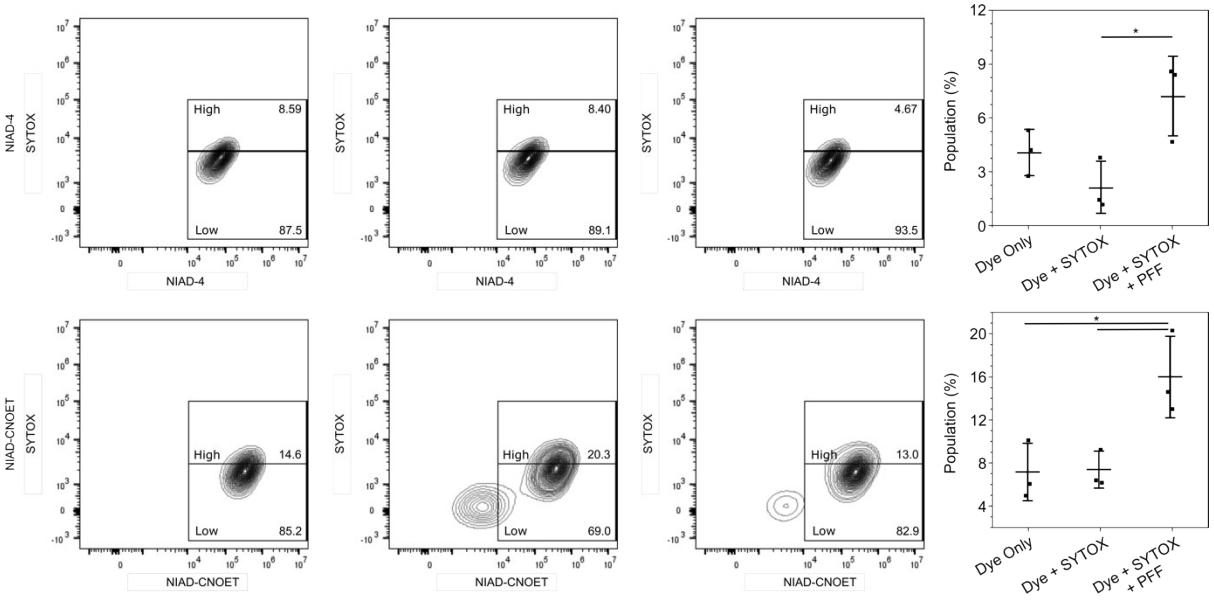

Figure S25: Flow cytometry gating strategy for n = 3 technical replicates for PFF treated cells stained by (top) NIAD-4 and (bottom) NIAD-CNOET with SYTOX as the counter stain. The high populations under different conditions are compared.

5. ^{1}H and ^{13}C NMR Spectra for compounds

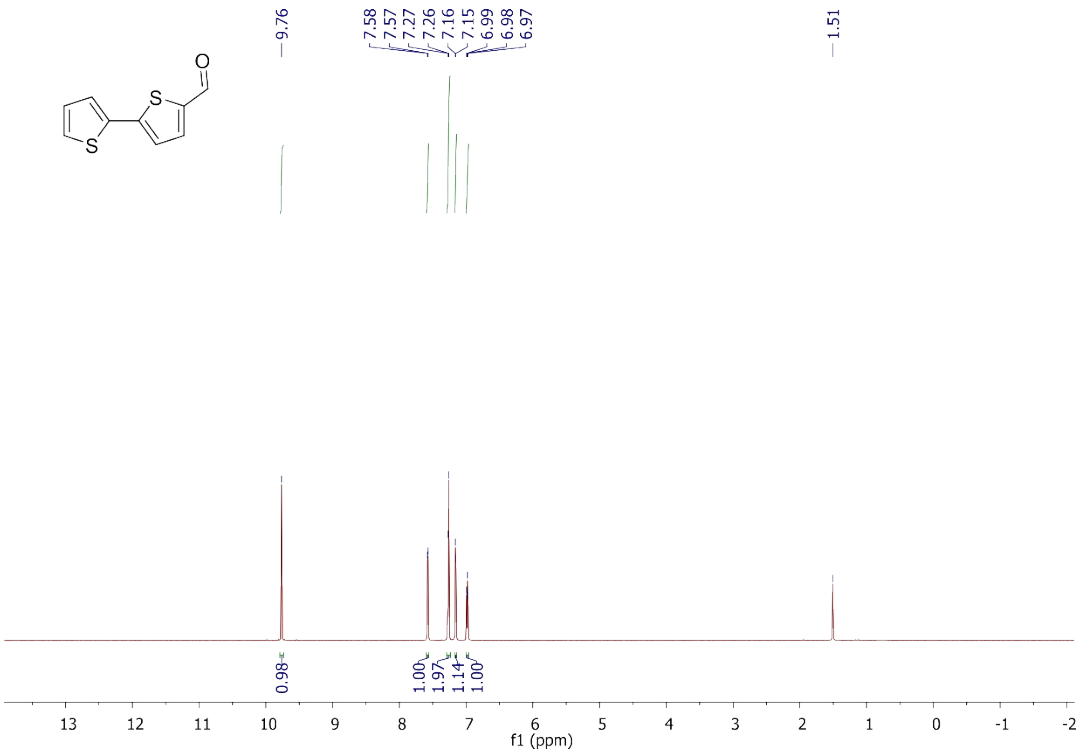

Figure S26: ^{1}H NMR of **1** in $CDCl_3$.

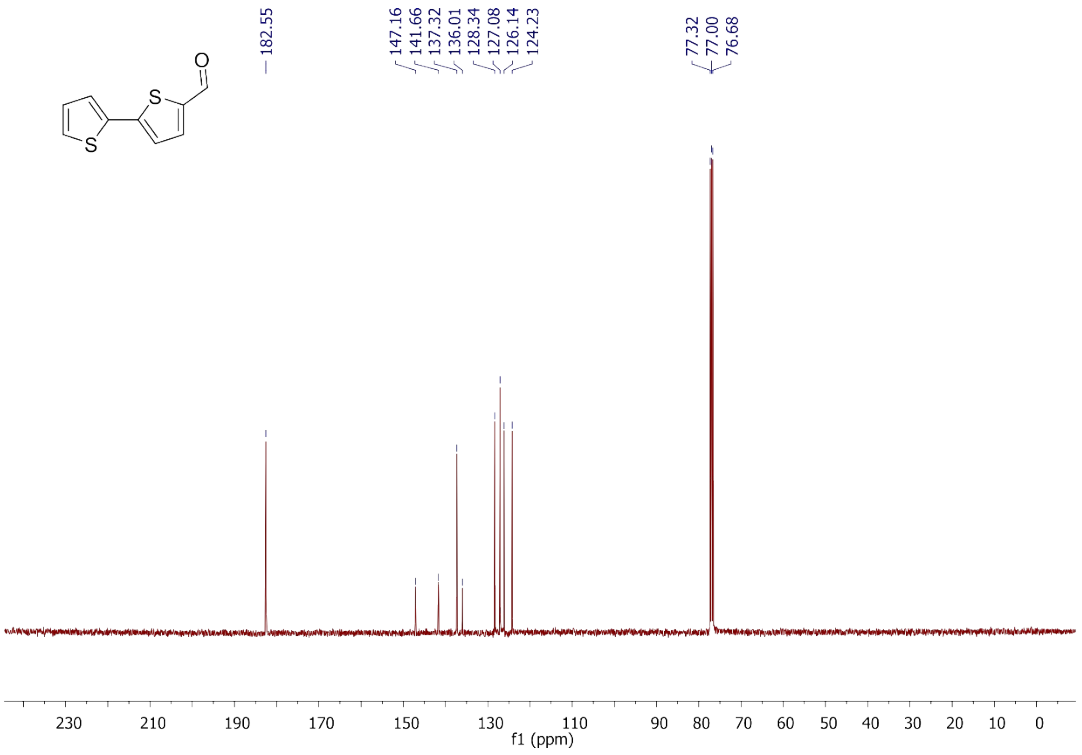

Figure S27: ^{13}C NMR of **1** in $CDCl_3$.

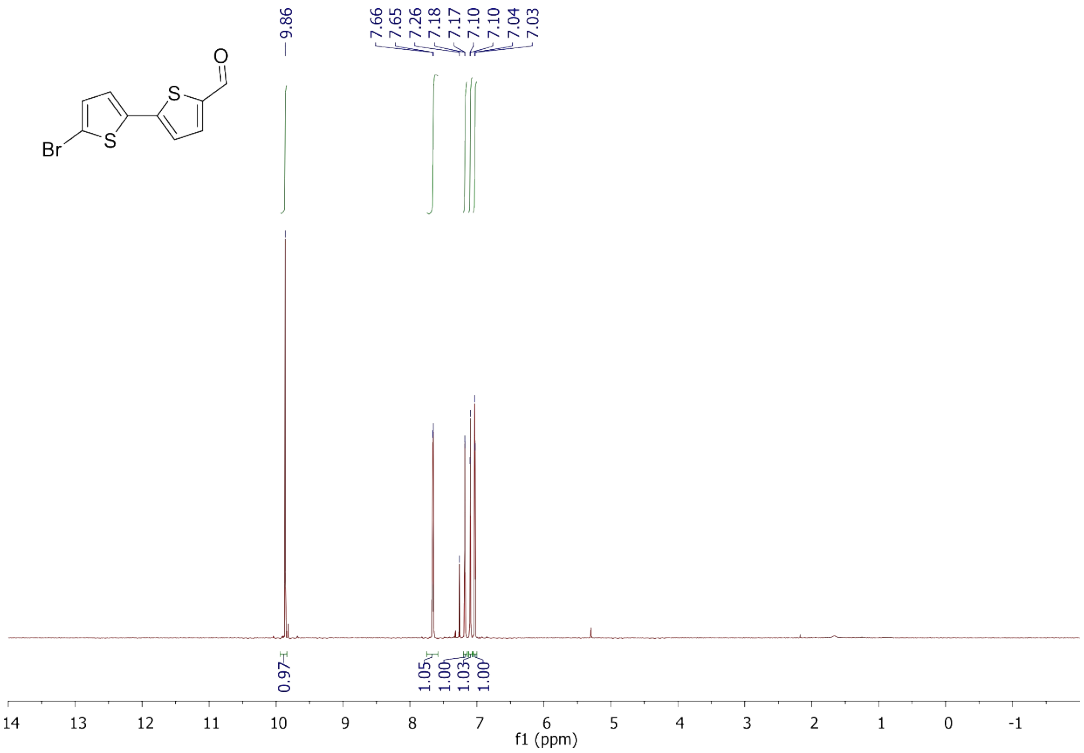

Figure S28: ^{1}H NMR of **2** in $CDCl_3$.

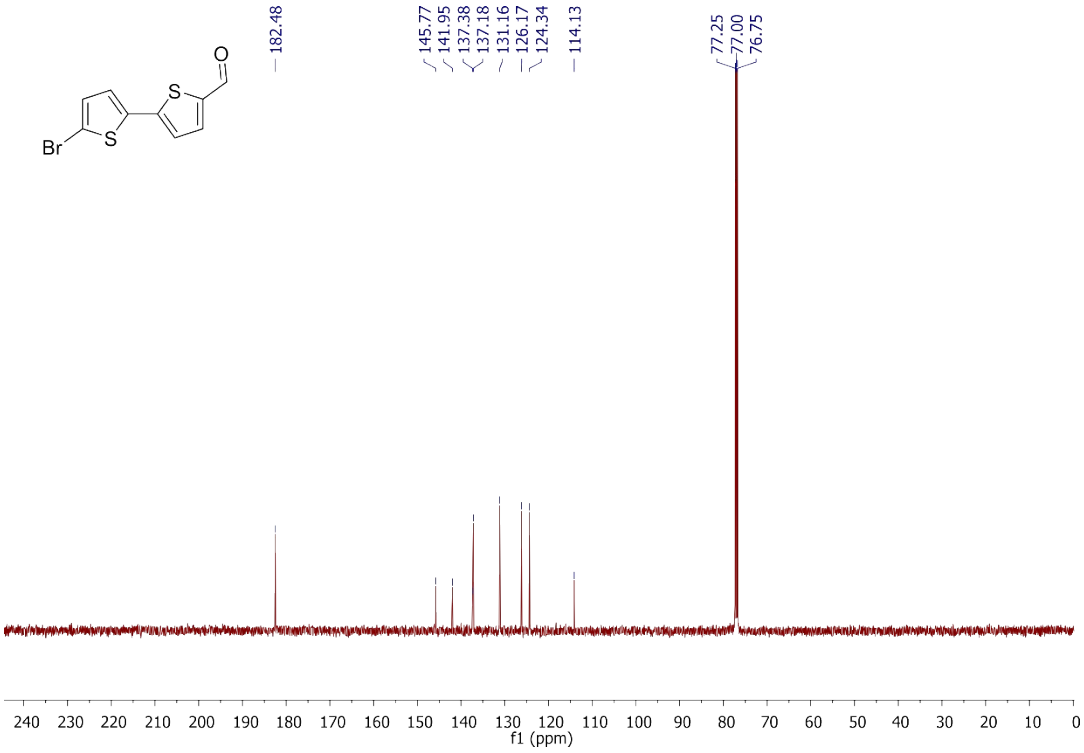

Figure S29: ^{13}C NMR of 2 in $CDCl_3$.

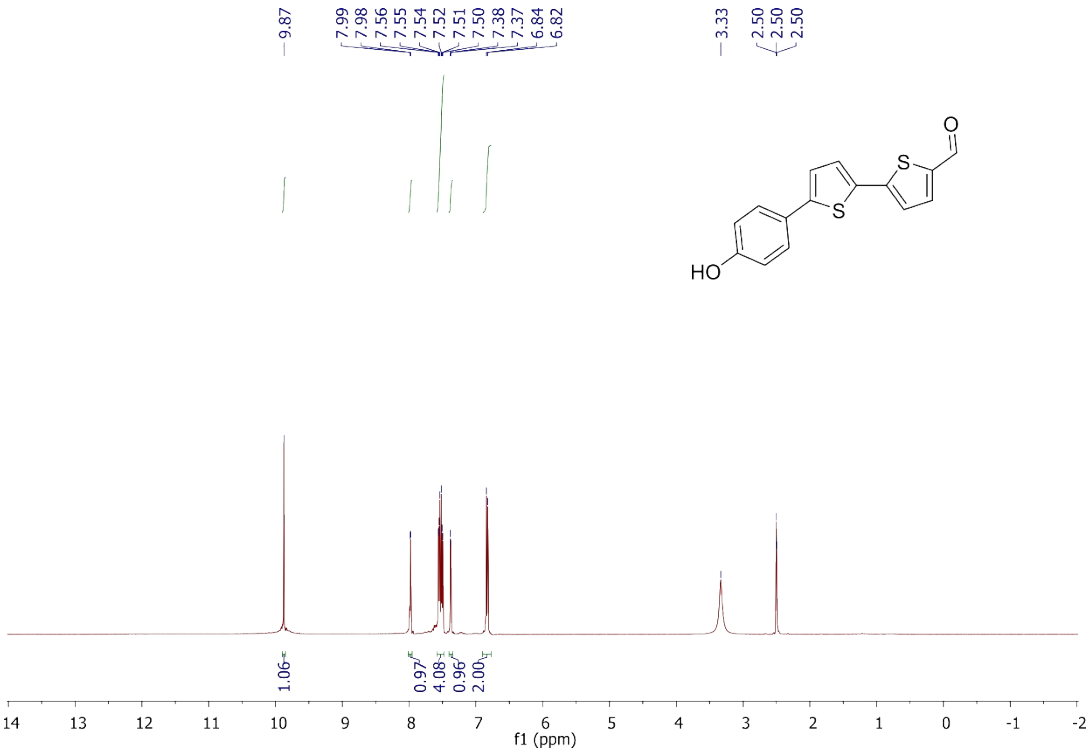

Figure S30: ^{1}H NMR of **3** in DMSO.

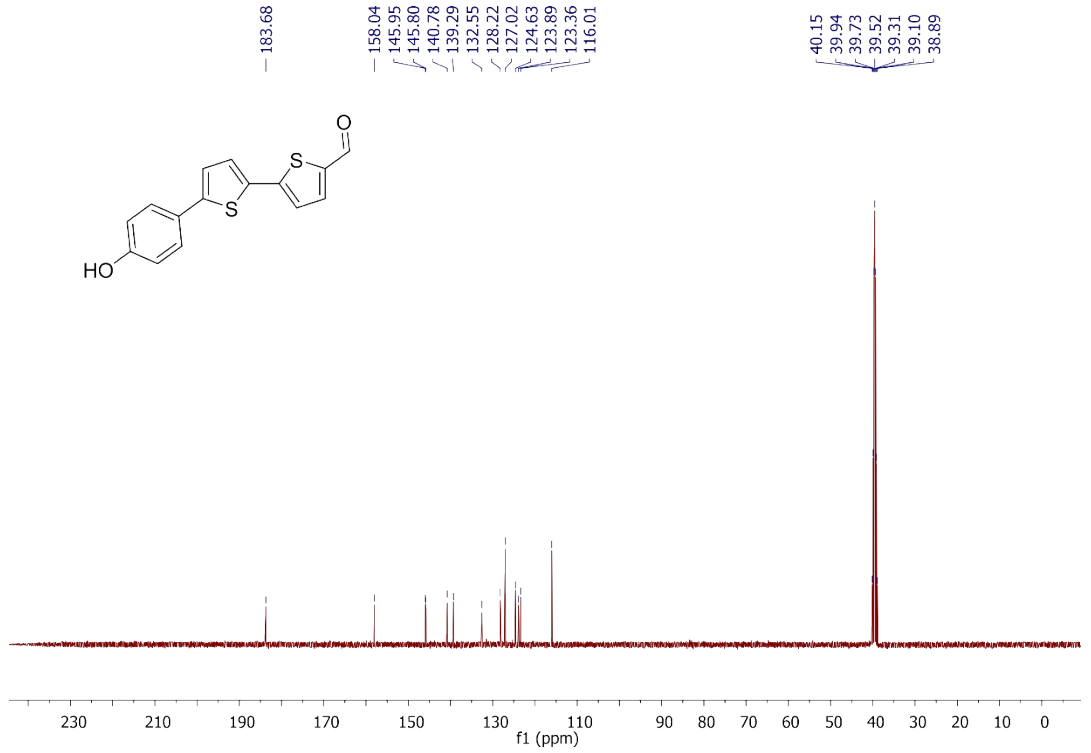

Figure S31: ^{13}C NMR of **3** in DMSO.

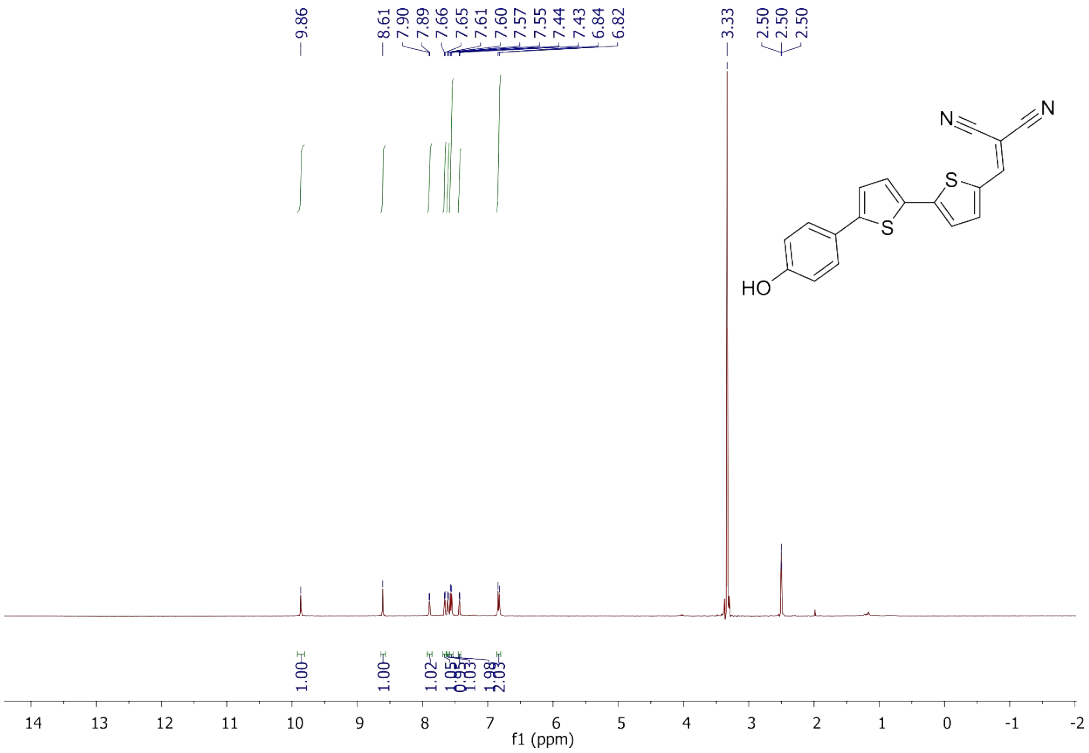

Figure S32: [1]H NMR of **NIAD-4** in DMSO.

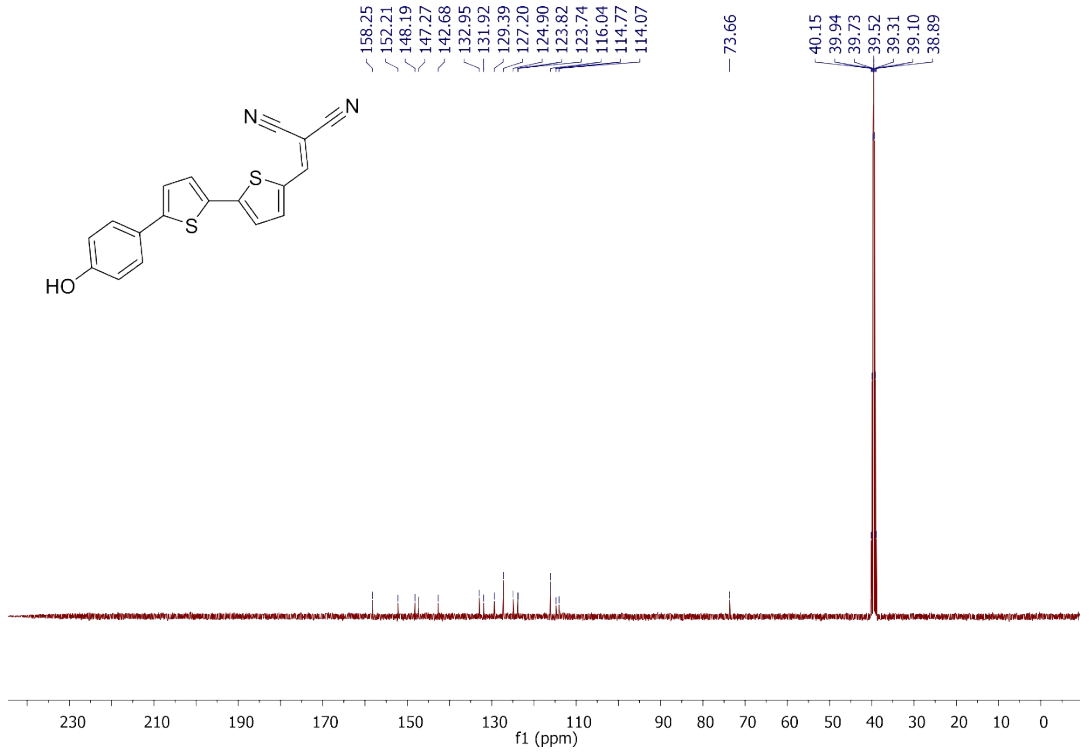

Figure S33: [13]C NMR of **NIAD-4** in DMSO.

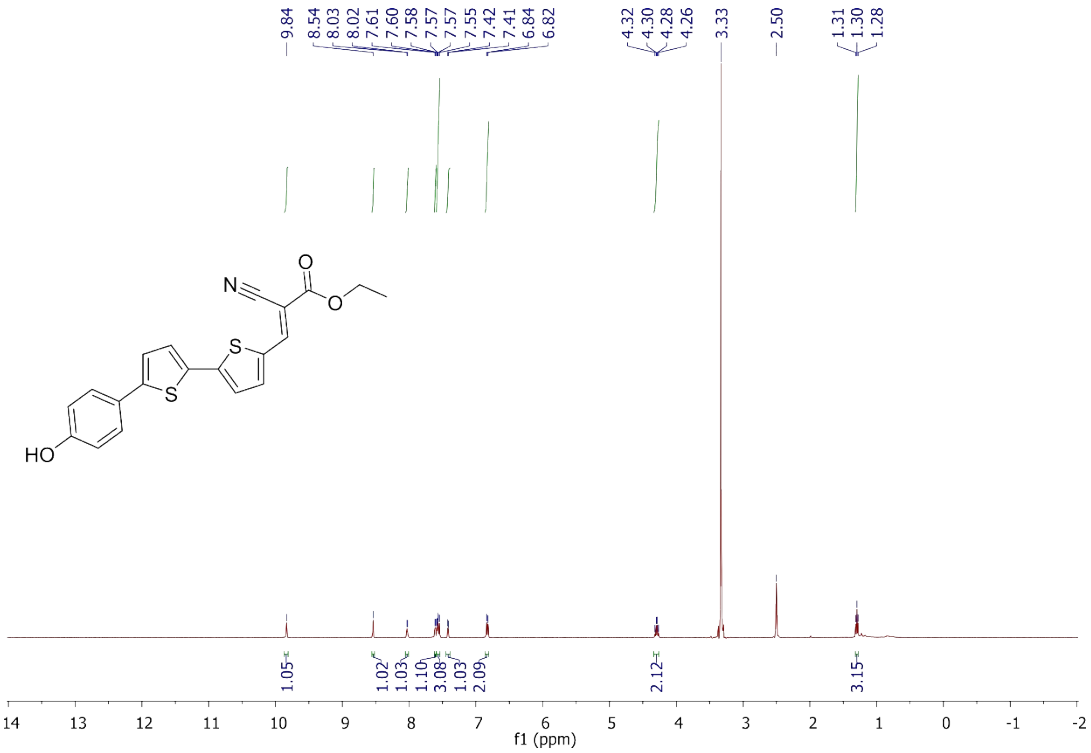

Figure S34: ^{1}H NMR of **NIAD-CNOET** in DMSO.

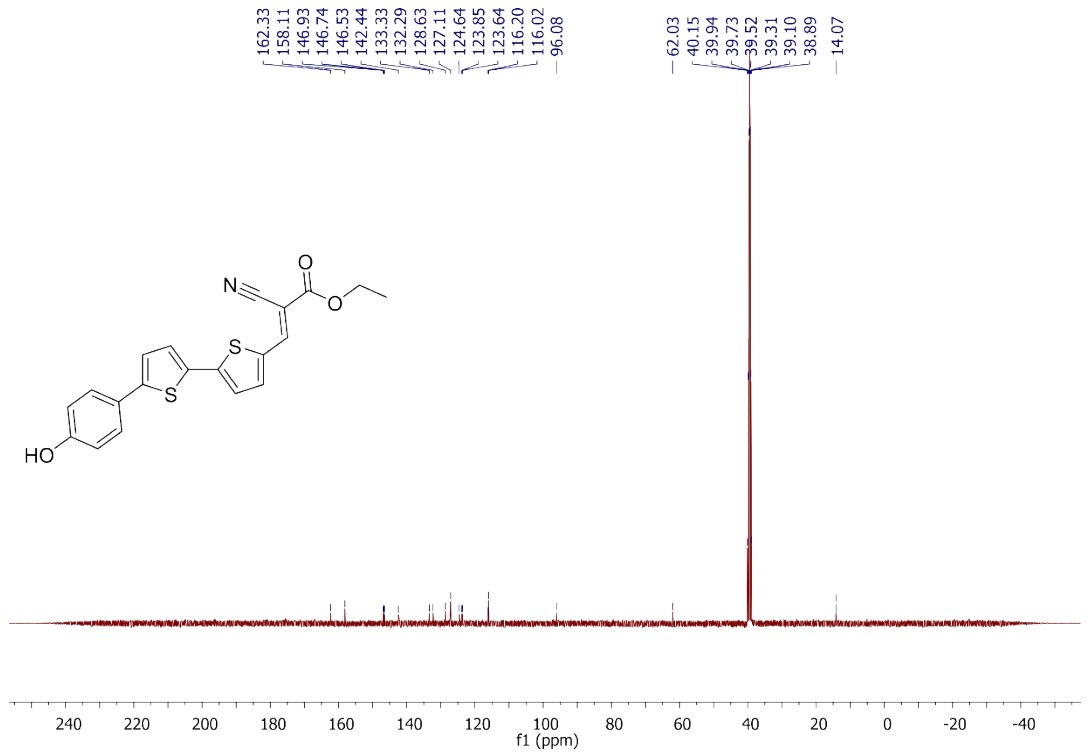

Figure S35: ^{13}C NMR of **NIAD-CNOET** in DMSO.

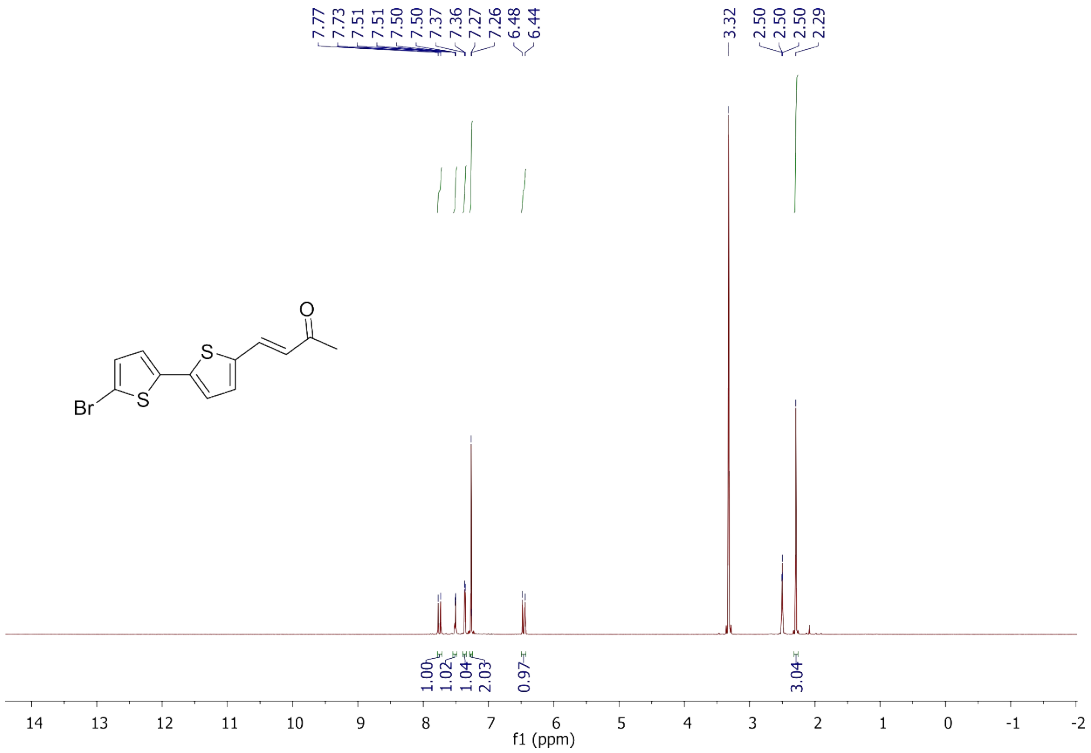

Figure S36: ^{1}H NMR of **4** in DMSO.

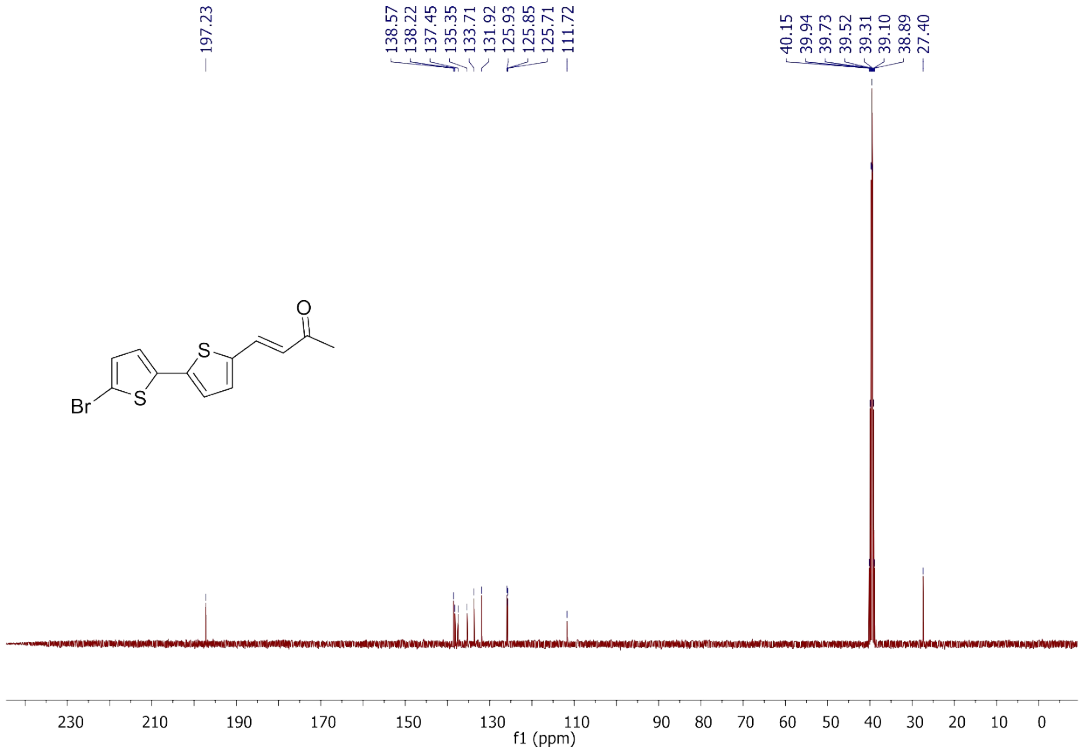

Figure S37: ^{13}C NMR of **4** in DMSO.

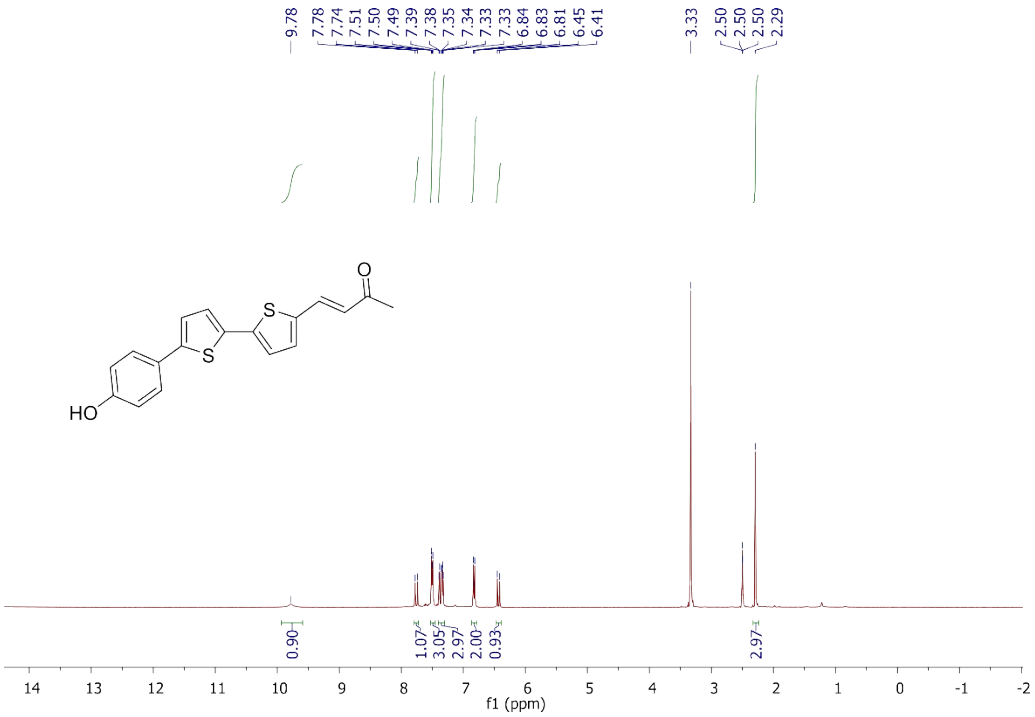

Figure S38: ^{1}H NMR of **ASV-NIAD** in DMSO.

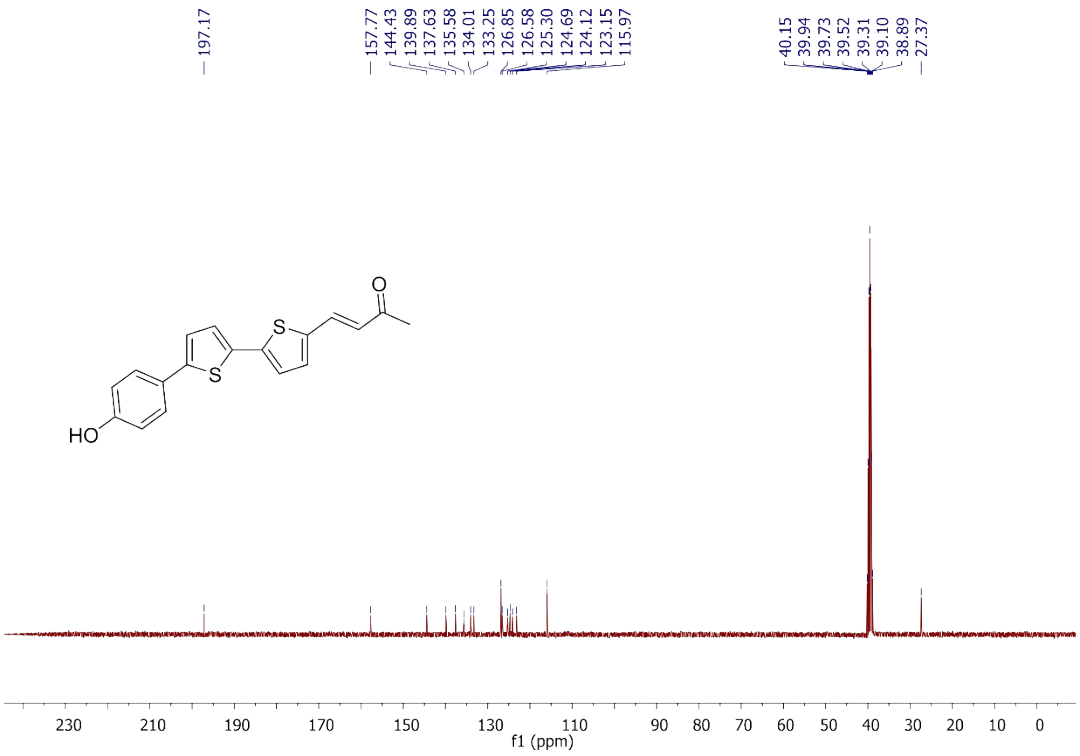

Figure S39: ^{13}C NMR of **ASV-NIAD** in DMSO.

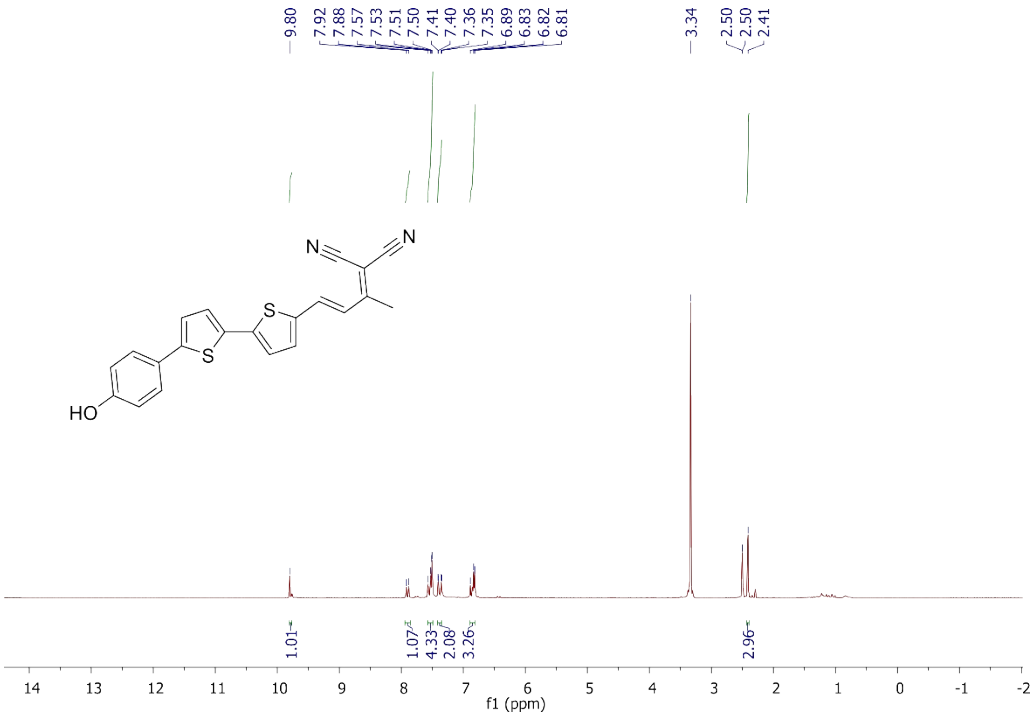

Figure S40: ^{1}H NMR of **ASC-NIAD** in DMSO.

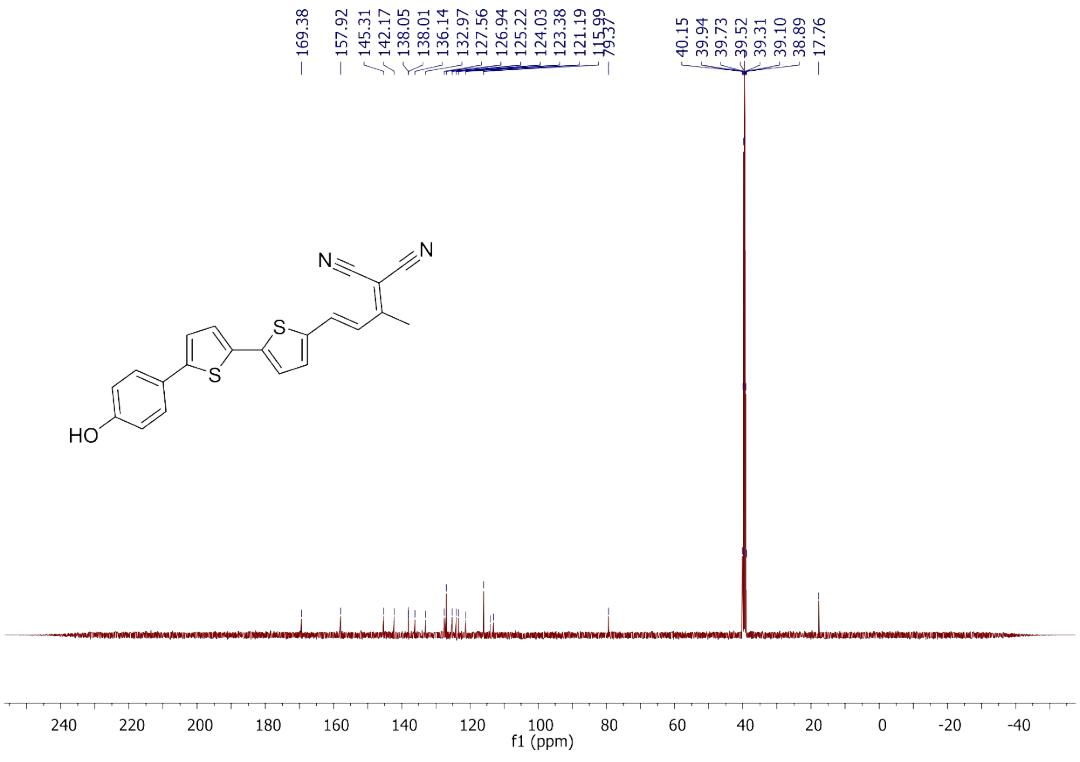

Figure S41: ^{13}C NMR of **ASC-NIAD** in DMSO.